# Phenotypic and Genotypic Consequences of CRISPR/Cas9 Editing of the Replication Origins in the rDNA of *Saccharomyces cerevisiae*

**Joseph C. Sanchez,*,†,‡,1 Anja Ollodart,*,† Christopher R. L. Large,*,† Courtnee Clough,*,† Gina M. Alvino,* Mitsuhiro Tsuchiya,§ Matthew Crane,§ Elizabeth X. Kwan,* Matt Kaeberlein,*,†,§ Maitreya J. Dunham,*,† M. K. Raghuraman,* and Bonita J. Brewer*,†,1,2**

*Department of Genome Sciences, †Molecular and Cellular Biology Program, and §Department of Pathology, University of Washington, Seattle, Washington 98195 and ‡Bioscience Division, Los Alamos National Laboratory, Los Alamos, New Mexico 87544

ORCID IDs: 0000-00002-2444-1834 (J.C.S.); 0000-0002-6329-9463 (A.O.); 0000-0002-5732-970X (C.R.L.); 0000-0002-7859-7252 (C.C.); 0000-0002-1311-3421 (M.K.); 0000-0001-9944-2666 (M.J.D.); 0000-0003-2382-3707 (M.K.R.); 0000-0001-8782-0471 (B.J.B.)

**ABSTRACT** The complex structure and repetitive nature of eukaryotic ribosomal DNA (rDNA) is a challenge for genome assembly, thus the consequences of sequence variation in rDNA remain unexplored. However, renewed interest in the role that rDNA variation may play in diverse cellular functions, aside from ribosome production, highlights the need for a method that would permit genetic manipulation of the rDNA. Here, we describe a clustered regularly interspaced short palindromic repeats (CRISPR)/Cas9-based strategy to edit the rDNA locus in the budding yeast *Saccharomyces cerevisiae*, developed independently but similar to one developed by others. Using this approach, we modified the endogenous rDNA origin of replication in each repeat by deleting or replacing its consensus sequence. We characterized the transformants that have successfully modified their rDNA locus and propose a mechanism for how CRISPR/Cas9-mediated editing of the rDNA occurs. In addition, we carried out extended growth and life span experiments to investigate the long-term consequences that altering the rDNA origin of replication have on cellular health. We find that long-term growth of the edited clones results in faster-growing suppressors that have acquired segmental aneusomy of the rDNA-containing region of chromosome XII or aneuploidy of chromosomes XII, II, or IV. Furthermore, we find that all edited isolates suffer a reduced life span, irrespective of their levels of extrachromosomal rDNA circles. Our work demonstrates that it is possible to quickly, efficiently, and homogeneously edit the rDNA origin via CRISPR/Cas9.

**KEYWORDS** rDNA copy number; fitness; replicative life span; origins of replication; turbidostat

WHILE the role of ribosomal DNA (rDNA) in ribosome production is uncontested, there has been renewed interest in exploring the role that rDNA variation may play in cell cycle regulation, life span, and cancer (Wang and Lemos 2017; Parks *et al.* 2018) . Because ribosomal content is one of the dominant components of cellular biomass, ribosomal RNA (rRNA) transcription imposes significant constraints on the speed with which cells can divide. The heavy transcriptional burden placed on the rDNA has necessitated large numbers of repeated units to cope with the demand for rRNAs. This burden, and the inherently repetitive nature of these sequences, can result in variation within an otherwise isogenic population. However, variation in the sequence or copy number of rDNA repeats has been difficult to assess experimentally (McStay 2016). Even though whole-genome sequencing (WGS) data are available for hundreds to thousands of different eukaryotes, the large sizes of the repeated, homogeneous, tandem structures make identifying and testing


doi: https://doi.org/10.1534/genetics.119.302351
Manuscript received May 22, 2019; accepted for publication June 28, 2019; published Early Online July 10, 2019.
Available freely online through the author-supported open access option.
Supplemental material available at FigShare: https://doi.org/10.25386/genetics.8162111.
[1]These authors contributed equally to this work.
[2]Corresponding author: Department of Genome Sciences, Box 355065, University of Washington, 3720 15th Ave. NE, Seattle, WA 98195-5065. E-mail: bbrewer@gs.washington.edu

sequence and copy number variants challenging in most species. The copy number of repeats can be highly variable from individual to individual (Stults *et al.* 2008; Xu *et al.* 2017) and are often difficult to reliably determine when orthogonal methods, such as digital droplet PCR or quantitative PCR (qPCR), quantitative hybridization, and WGS read-depth measurements give variable estimations of copy number from the same DNA sample (Xu *et al.* 2017; Chestkov *et al.* 2018). Adding to the complexity of the problem is the fact that, in many eukaryotes, the rDNA is also found on multiple chromosomes. Directed mutational analysis, a technique so powerful for analyzing single-copy sequences, has not been a realistic option in the rDNA of most organisms because of the difficulty in mutagenizing all of the repeats simultaneously. Therefore the systematic testing of individual sequence or copy number variants has been genetically intractable.

In the budding yeast *Saccharomyces cerevisiae*, limited mutational analysis of the rDNA locus has been carried out by taking advantage of a recessive hygromycin-resistant mutation (T to C) at position 1756 of the 18S rRNA. When this variant rDNA repeat is introduced into yeast on a multicopy plasmid, cells can become hygromycin-resistant by deleting most or all of the chromosome XII copies of the rDNA (Chernoff *et al.* 1994; Wai *et al.* 2000), and relying on the plasmid copies of the rDNA for ribosome production. Using a plasmid-shuffle protocol or direct reintegration of sequences into chromosome XII, researchers can examine the consequences of mutated rDNA elements. This basic protocol has been used to explore transcriptional regulatory elements of the Polymerase I (PolI) promoter and enhancer (Wai *et al.* 2000), the role of expansion segments in ribosome fidelity (Fujii *et al.* 2018), the sequence requirements for replication-fork blocking at the 3′-end of the 35S transcription unit (the replication fork barrier, RFB) (Ganley *et al.* 2009; Saka *et al.* 2013), and on a more limited scale, the requirements for the rDNA origin of replication in copy number expansion (Ganley *et al.* 2009). While these experiments are elegant, there are problems with interpreting the resultant phenotypes; in particular, the introduction of altered rDNA sequences requires the simultaneous introduction of a selectable marker that becomes part of each of the amplified variant rDNA repeats.

Here, we edited the yeast rDNA locus directly without the introduction of a selectable marker by using clustered regularly interspaced short palindromic repeats (CRISPR)/Cas9 (Doudna and Charpentier 2014). Our method to mutagenize rDNA was developed independently but is similar to one previously reported (Chiou and Armaleo 2018) which was intended for a different biological purpose. We altered the origin of replication that is found in each repeat by deleting it entirely, or by replacing the 11-bp A+T-rich origin consensus sequence with a G+C block or other functional origins. We describe our protocol for editing the rDNA, characterize the surviving clones, and propose a mechanism by which transformants are able to successfully replace multiple tandem repeats. Among the surviving transformants complete sequence replacements are frequent and easily detected. In addition, we analyzed the phenotypic consequence of altering the sequence of the rDNA origin.

We find that deletion of the rDNA origin limits the number of rDNA repeats that can be maintained by passive replication—*i.e.*, by a fork from an origin in the flanking non-rDNA region—to ∼10. The resulting limitation on ribosome production creates a strong selective pressure for suppressors of the slow-growth phenotype. Using multiple, long-term growth regimes, we find that suppressors arise through segmental aneusomy of the region of chromosome XII that contains the rDNA locus or through aneuploidy of chromosomes XII, II, or IV. Replacing the rDNA origin with other functional origins or reintroducing the rDNA origin also leads initially to reduced rDNA copy number. Over ∼140 generations, the locus reexpands but does not reach the initial ∼150 copies. All strains that survived CRISPR editing at the rDNA locus showed a reduction in life span that is unrelated to the level of extrachromosomal rDNA circles (ERCs), which we found can vary among the strains by ∼100-fold. Our genetic analysis of this understudied, essential, complex locus in yeast adds critical understanding regarding the consequences of rDNA origin variation.

## Materials and Methods

### *Strains, growth medium, plasmids, and PCR*

All edited strains were derived from BY4741 or BY4742. Strains were verified by PCR, restriction digestion, and/or Sanger sequencing of the PCR products. Cells were grown at 30° in defined synthetic complete medium with or without uracil (for selection of the Cas9 plasmids), and supplemented with 2% dextrose.

pML104 (pML104; Laughery *et al.* 2015) was purchased from Addgene, and cleaved sequentially with *Bcl*I and *Swa*I. Complementary oligonucleotides for each of the guide sequences were annealed and ligated into cut pML104. Colonies were selected on LB ampicillin plates and transformants were Sanger sequenced. Multiple-guide plasmids were Gibson-assembled (Gibson 2011) from PCR products of single-guide plasmids.

### *Creating and characterizing the CRISPR/Cas9-edited rDNA arrays*

To maximize the cutting potential of the system, we cloned multiple guides into a single plasmid (pML104; Laughery *et al.* 2015) that contains the Cas9 gene, a *URA3* selectable marker, and the 2-μm origin of replication that stably maintains the plasmid at high copy number (pACD; Supplemental Material, Figure S1A). We designed a 250-bp "gBlock" repair template with mutations at four possible NGG protospacer adjacent motif (PAM) sequences (rendering the repair template resistant to Cas9 cleavage) and a G+C block that replaced the 11-bp A+T-rich autonomous replication sequence (ARS) consensus sequence (ACS; Figure 1A and Figure S1B). We transformed strain BY4741 with pML104 or

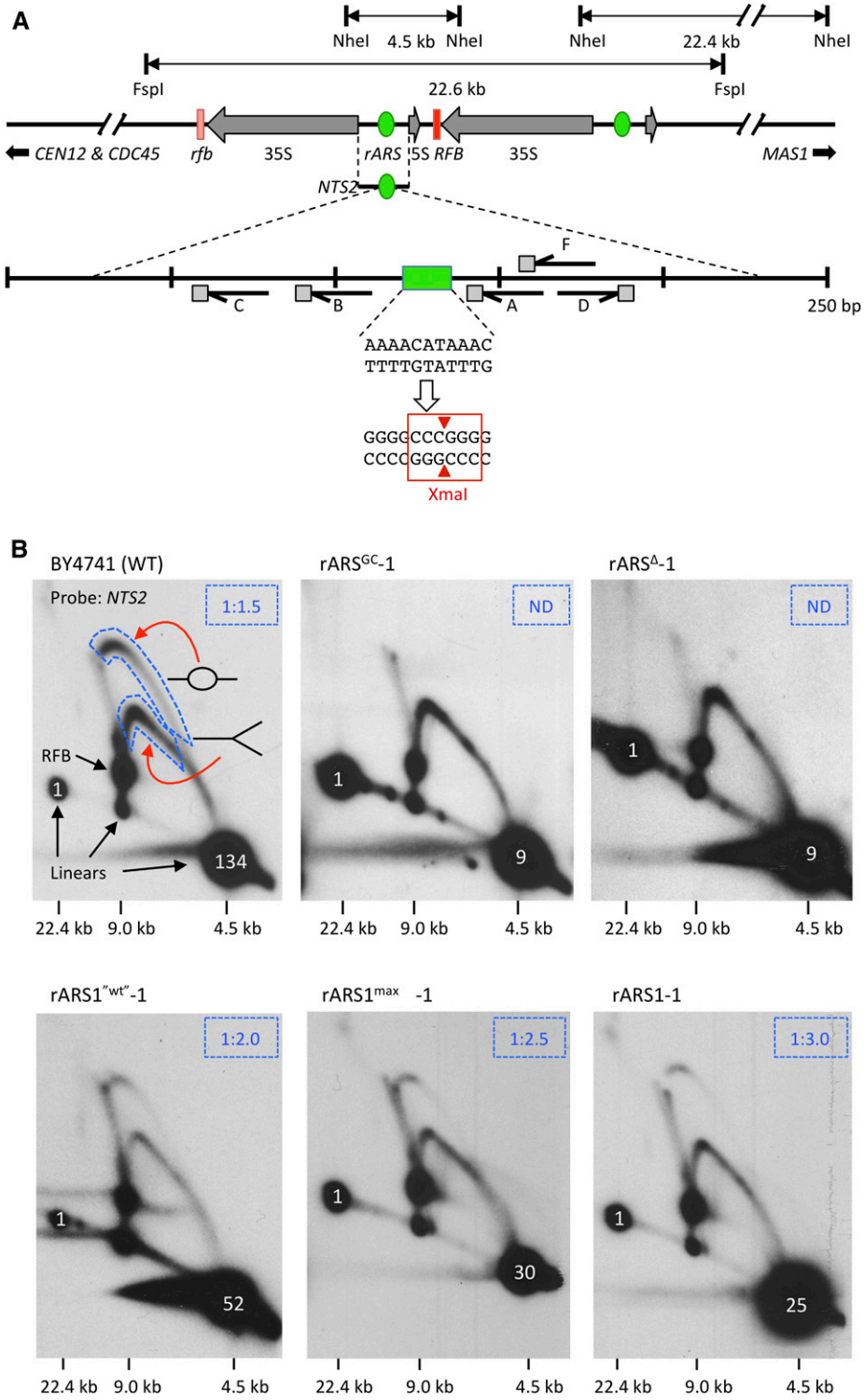


**Figure 1** Alterations to the rDNA origin and assessment of origin function. (A) A map of the rDNA locus adapted from the *Saccharomyces* Genome Database (https://www.yeastgenome.org) representing just two of the ~150 rDNA repeats in the reference yeast strain. *Nhe*I and *Fsp*I restriction sites relevant to this study are indicated, as well as the proximal (*CEN12* and *CDC45*) and distal (*MAS1*) sequences used for hybridization probes. The left RFB, indicated in light red, is a truncated version of the RFB that is present in all of the other repeats. The 250-bp region of *NTS2* that contains the origin of replication shows the elements targeted for alterations by CRISPR/Cas9. The A+T sequence of the *rARS* ACS (green box) was replaced by a G+C sequence that introduces an *Xma*I site. The half arrows indicate the guide RNA sequences and the gray squares indicate the NGG PAM sites. (B) rDNA origin function was assessed by 2D gel electrophoresis. DNA isolated in agarose plugs from asynchronously growing WT and edited strains was cleaved with *Nhe*I to release the *NTS2* fragment on a 4.5-kb fragment. Bubble-shaped molecules, indicative of initiation, are more retarded in the second dimension than Y-shaped molecules. We assessed initiation efficiency by comparing the intensity of the bubble arc relative to the Y arc (areas surrounded by dashed lines). The bubble:Y ratio is indicated in the upper right corner of each 2D gel. ND indicates that no signal above background was measured for the bubble region. Sizes of relevant linear species are indicated below each 2D gel panel. Numbers in white superimposed on the 4.5-kb fragments indicate the copy number estimated from the single-copy sequence at 22.4 kb. 2D, two-dimensional; ACS, ARS consensus sequence; ARS, autonomous replication sequence; CRISPR, clustered regularly interspaced short palindromic repeats; PAM, protospacer adjacent motif; rDNA, ribosomal DNA; RFB, replication fork barrier; WT, wild-type.

pACD, and included excess repair template in either single- or double-stranded form. While pML104 produced hundreds of Ura+ colonies per microgram of plasmid DNA within 3 days, transformation with pACD with or without repair template produced only dozens of colonies of variable sizes that appeared over the course of a week's incubation (Figure S2A). The reduced transformation efficiency is consistent with the assumption that unrepaired double-stranded breaks in the rDNA are lethal.

After restreaking the transformants on selective plates (Figure S2B), we characterized their rDNA loci by performing PCR, restriction digestion (Figure S2C), and/or sequencing (Figure S3). Transformation with the repair template along with pACD was expected to produce no change in size of the

PCR fragment if the target was edited correctly; however, the PCR product should contain an *Xma*I site that was absent in the original rDNA sequence (Figure 1A and Figure S1B). Four of the eight transformants that received pACD alone showed no signs of editing, and the other four clones yielded reduced or no PCR fragments, suggesting that they had suffered a deletion in the region (Figure S2C). Among a set of 16 transformants that received both pACD and the repair template, we found a single clone with the appropriate PCR fragment size and sensitivity to *Xma*I as expected for correct editing (transformant #6; pACD + single-stranded template; Figure S2C). The sequence of the PCR fragment revealed all four PAM mutations and the 11-bp G+C cassette (Figure S3A; refer to gBlock sequence in Table S1). The remaining transformants either failed to produce a PCR fragment or produced a shorter than expected PCR fragment, suggesting that they had suffered a deletion. We sequenced the PCR fragment from one of these clones (transformant #2; pACD + double-stranded template; Figure S2C) and found it to have a deletion that removed 167 bp of the origin region, including all guide RNA sites (Figure S3B and Table S1). We repeated the transformation experiments, focusing primarily on small transformant colonies, and obtained and characterized in detail additional *rARS*$^{GC}$ (rARS$^{GC}$-2) and *rARS*$^{\Delta}$ mutants (rARS$^{\Delta}$-2).

Editing of the rDNA repeats changed two features of the rDNA locus: the origin was removed and the copy number of the repeats was drastically decreased. To disentangle the phenotypes, we repeated the editing experiments using pACD, and a template with the wild-type rDNA origin and the four PAM site mutations. To detect introduction of *rARS*$^{\text{“}wt\text{”}}$, we took advantage of the fact that the sequence at two of the PAM sites could be distinguished by differential restriction enzyme digestion: an *Apo*I site is present at the edited PAM site associated with guide A and an *Hae*III site is present at the native PAM site associated with guide D (Figure S1B and Figure S4A). PCR and restriction digest analysis revealed that three of the clones (Figure S4A lanes 2, 3, and 12) had a successful replacement with the modified wild-type rARS. We refer to these strains as rARS$^{\text{“wt”}}$-2, rARS$^{\text{“wt”}}$-3, and rARS$^{\text{“wt”}}$-12.

To target *ARS1* or *ARS1*$^{max}$ to the rDNA locus, we included ~170 bp of nontranscribed spacer 2 (*NTS2*) homology flanking *ARS1* or *ARS1*$^{max}$ (Table S1). Using rARS$^{GC}$-1 as the starting strain, we cotransformed *ARS1*$^{max}$ and the single-guide RNA plasmid pF (Figure S1A). We expected successful repair using the *rARS1*$^{max}$ template to produce a larger PCR fragment that was missing the *Xma*I site but instead would contain a *Bsp*HI site (Figure S1B). More than 50% of the slow-growing clones contained the desired ARS replacements (Figure S4B). We were also able to recover, at high efficiency, the *ARS1* or *ARS1*$^{max}$ replacements using plasmid pACD, and BY4741 as the starting strain (Figure S4C). *ARS1* replacements produce the same larger-sized PCR fragment that contains a novel *Bgl*II site (Figure S1B and Figure S4C).

### *CHEF and two-dimensional gel electrophoresis*

For CHEF gel analysis of chromosome sizes, 1–1.5 ml of saturated yeast cultures were embedded in 0.5% GTG (Genetic Technology Grade) agarose plugs and processed as described (Kwan *et al.* 2016). We used three CHEF gel running conditions in a CHEF DRII (Bio-Rad, Hercules, CA): the full chromosome run (which separates all chromosomes except for IV and XII) was 64 hr in 0.8% low electroendosmosis (LE) agarose with 0.5× TBE at 165 V, with switch times from 47 to 170 sec; the rDNA run (which separates larger chromosomes, such as IV and XII) was 68 hr in 0.8% LE agarose with 0.5× TBE at 100 V, with switch times from 300” to 900”; the *Fsp*1-digested chromosomes were run as for the full chromosome run but for only 44 hr. To collect DNA for two-dimensional (2D) gels, cells were grown to midlog phase, quick chilled in 0.1% (w/v) sodium azide and 200 mM EDTA, and concentrated by centrifugation. Agarose plugs from frozen cell pellets were prepared by the protocol available at http://fangman-brewer.gs.washington.edu. Methods for restriction digestion of DNA in plugs and conditions for 2D gel electrophoresis of rDNA replication intermediates can be found in Sanchez *et al.* (2017). Southern transfer and hybridization with $^{32}$P-dATP PCR-amplified probes were performed according to standard protocols. The split Southern/northern gel was performed as described in Sanchez *et al.* (2017).

### *Turbidostat growth*

Turbidostats were constructed and run under software from McGeachy *et al.* (2019). Samples were harvested at the indicated times by collecting the effluent on ice over a ~15-min interval. Custom R scripts were used to convert the calculated influent amount to a doubling time.

Run 1 parameters: four separate colonies, two each of rARS$^{GC}$-1 (colonies a and b) and rARS$^{\Delta}$-1 (colonies a and b), were grown in WFC medium. Each 200-ml turbidostat was inoculated with 2 ml of an overnight culture. The cells were then allowed to grow until they reached $OD_{600} \approx 1$. At this point, another sample was taken to manually measure the $OD_{600}$ of the cells, which was then used to calibrate the turbidostat readings. The turbidostat was then set to maintain a constant $OD_{600}$ of 1. At the same time each day, 15 ml of effluent from each turbidostat was collected on ice (~10–15 min). Cells were pelleted at 4000 × *g* for 5 min and frozen at −20° for downstream analysis. Glycerol stocks of 1 ml were also collected and stored at −80°.

Run 2 parameters: the $OD_{600}$ was set to 0.5 to more accurately reflect log phase growth, and 50-ml samples of cells were collected to account for the decreased density and to provide adequate samples for additional assays.

For doubling-time analysis, the system measures the on/off cycling of the media pump that is delivering medium at a known rate. A custom R script fits a line to the change in the overall time the pump is on over a 2-hr window. The slope of that line is then scaled by the known flow rate and volume of the vessel. This calculation produces a doubling time for that 2-hr interval.

### Replicative life span analysis

Yeast replicative life spans were performed as previously described (Kaeberlein *et al.* 2004). Briefly, strains were streaked from frozen stocks onto YEP glycerol media plates to minimize the chance of copy number change in the rDNA. Strains were then patched onto YEP dextrose plates where they were allowed to grow for several generations. Virgin daughters were isolated, allowed to grow into mothers, and then individual daughters were manually removed. Each division of the mother cell was recorded until the mother cells failed to divide. Statistical significance was determined using Wilcoxon rank-sum analysis.

### WGS

Total cellular DNAs from rARS$^{GC}$-1a and -1b samples were isolated from stationary-phase yeast cultures by standard methodology (Hoffman and Winston 1987). DNA was fragmented by Covaris sonication (450 peak factor, 30% duty factor, and 200 cycles per burst) prior to single-index library construction using the KAPA Hyper Prep Kit. Following qPCR for quality control and quantification, libraries were sequenced on an Illumina NextSeq 500 using the manufacturer's recommended protocols.

Libraries from the turbidostat cultures were prepared by isolating genomic DNA using the Hoffman–Winston protocol (Hoffman and Winston 1987). DNA concentration was assessed using Qbit. Aliquots of genomic DNA (50 ng) were prepared with the Nextera Library kit, according to the kit's instructions.

### Alignment and SNP/insertion/deletion variant calling

WGS reads were aligned using Bowtie2 (Bowtie/2.2.3) (Langmead and Salzberg 2012) or BWA-mem (BWA/0.7.15) (Li 2013) to the sacCer3 reference genome (Engel *et al.* 2014) depending on read length (BWA for $>$ 100 bp and Bowtie2 for $<$ 100 bp), then sorted and indexed using SAMtools/1.9 (Li *et al.* 2009). Duplicates were marked and removed using Picard tools (picard/2.6.0), resorted, and indexed using SAMtools. The insertion/deletions in the alignments were realigned using the GATK/3.7 package. Variants were called using freebayes/1.0.2-6-g3ce827d (Garrison and Marth 2012) with modified arguments (–pooled-discrete–pooled-continuous–report-genotype-likelihood-max–allele-balance-priors-off–min-alternate-fraction 0.1) and LoFreq/2.1.2 (Wilm *et al.* 2012) in a paired mode with their genetic ancestor. Called variants were filtered for uniqueness against their genetic ancestor(s) using bedtools/2.26.0. The variants were filtered for quality using bcftools/1.9 (Table S3). The filtered variants were annotated (Pashkova *et al.* 2013) and manually inspected for accuracy using the Interactive Genomics Viewer (IGV) (Robinson *et al.* 2011).

### Copy number and rearrangement analysis

Using 1000-bp sliding windows (IGVtools), normalized by the mean total read depth across the genome (GATK/3.7), the copy number was plotted and manually inspected for changes in copy number with the sample's genetic ancestor. Copy number change breakpoints were manually inspected to determine the type of rearrangement using split and discordant reads, generated with BWA-mem (Li 2013), SAMBLASTER/0.1.24 (Faust and Hall 2014), and SAMtools.

### Data availability

All WGS data have been deposited at https://www.ncbi.nlm.nih.gov/sra with the bioproject accession number PRJNA544115 and will be made publicly available upon publication of the article. All other data necessary for confirming the conclusions of this article are fully within the article, its tables and figures, or in the supplemental material. Yeast strains are available upon request. Supplemental material available at FigShare: https://doi.org/10.25386/genetics.8162111.

## Results

### Altering the replication origins in the yeast rDNA locus using CRISPR/ Cas9

Each repeat in the rDNA locus of *S. cerevisiae* contains a potential origin of replication between the divergently transcribed 35S and 5S genes in a region designated *NTS2* (Figure 1A). This origin sequence is inefficient in its native location (in many of the repeats the origin does not participate in replication initiation) (Brewer and Fangman 1988; Muller *et al.* 2000; Pasero *et al.* 2002) and plasmids that contain the rDNA origin as their ARS are poorly maintained (Larionov *et al.* 1984; Miller *et al.* 1999; Kwan *et al.* 2013). To determine whether the origin is essential for any of the diverse rDNA functions, we set out to use the CRISPR/Cas9 system to edit the entire set of repeats (see *Materials and Methods*, Figure S1A). We replaced the endogenous 11-bp A+T-rich ACS (Figure 1A, Figure S1B, and Table S1) with a G+C block that contains four potential NGG PAM site alterations. We called these transformants rARS$^{GC}$-1 and -2, and refer to their rDNA origins as *rARS$^{GC}$* (Figures S2 and S3A). We also characterized two deletions that removed the origin region including all guide RNA sites (Figures S2 and S3B, and Table S1). We called these strains rARS$^{\Delta}$-1 and -2, and refer to their rDNA origins as *rARS$^{\Delta}$*.

To introduce alternate origins into the rDNA, we repeated the editing experiments, this time either introducing non-rDNA origins or reintroducing the wild-type rDNA origin. We chose two versions of the chromosome IV origin *ARS1* to replace the rDNA origin: a 100-bp fragment of the wild-type version of *ARS1* and a multiply substituted version of *ARS1*, called *ARS1$^{max}$*, that contains ~50 mutations discovered through a deep mutational scan, each of which contributed to improved plasmid maintenance (Liachko *et al.* 2013; Figure S1B and Table S1). We refer to these strains as rARS1-# and rARS1$^{max}$-#. As a control for editing efficiency, we also reintroduced the wild-type rDNA origin and the four PAM site mutations. We refer to these strains with the edited *rARS"wt"*

as rARS"wt"-2, rARS"wt"-3, and rARS"wt"-12. Based on molecular analyses of the transformant clones (Figures S2, S3, and S4), we conclude that the editing of the entire set of rDNA origins is both efficient and complete.

### Assessment of origin function in strains with modified rDNA origins

To confirm that the modifications to the rARSs had altered origin functions, we collected asynchronously growing cultures to analyze replication intermediates by 2D gel electrophoresis (Brewer and Fangman 1987). We digested chromosomal DNA with *Nhe*I to examine a ~4.5-kb fragment that contains the rDNA origin near its center (Figure 1A). We hybridized the Southern blots of the 2D gels with the *NTS2* probe looking for evidence of bubble structures that would signal initiation within the fragment (Figure 1B). BY4741 produces the standard pattern of bubbles and Ys in a ratio of ~1:1.5, a ratio that indicates that around one out of every two-to-three repeats has an active origin and that the other adjacent repeats are passively replicated by a fork from the upstream active origin. We found no bubbles among the replication intermediates for the rDNA loci in rARS$^{GC}$-1 and rARS$^{\Delta}$-1, only Ys that were produced through passive replication (Figure 1B). We conclude that the GC replacement and the deletion of the rARS reduce initiation efficiency in the rDNA below the level of detection by this assay. The 2D gel analysis of strains with *rARS"wt"*, *ARS1$^{max}$*, and *ARS1* replacements showed that these origins are functional after reintroduction into *NTS2* although the levels of replication initiation were somewhat lower than for the parent BY4741 strain; one out of every three-to-four repeats has an active origin (Figure 1B).

A second feature revealed by the 2D gel analysis was a drastic change in copy number of the rDNA after origin editing. The telomere-proximal junction between the rDNA and unique sequences produces a 22.4-kb *Nhe*I fragment that also contains the *NTS2* sequence (Figure 1A). By comparing the intensity of hybridization of the 4.5-kb *NTS2* linear fragment to this junction fragment, we determined that this particular isolate of BY4741 has ~134 rDNA repeats, while both rARS$^{GC}$-1 and rARS$^{\Delta}$-1 have around nine copies (Figure 1B). Including a functional ARS on the repair template produced transformants with repeat numbers that were higher, but significantly lower than those of the BY4741 parent (Figure 1B).

### Phenotypic properties of strains with modified rDNA origins

rARS$^{GC}$-1 and rARS$^{\Delta}$-1 were slow to come up on the transformation plates, and maintained their slow growth upon restreaking (Figure S2B). They were still able to utilize glycerol as the sole carbon source, ruling out a respiratory defect as the cause of slow growth. The same was true for all of the transformants that yielded smaller or no *NTS2* PCR fragments. Those transformants that escaped editing by Cas9 grew significantly faster (Figure S2B), and by avoiding the largest colonies on transformation plates in subsequent experiments we were able to bias recovery of edited clones. In liquid synthetic complete medium, *rARS$^{GC}$* and *rARS$^{\Delta}$* variants maintained their slow growth. In comparison to the 90–100-min doubling time for BY4741, rARS$^{\Delta}$-1 had a doubling time of ~195 min and rARS$^{GC}$-1 grew with a slightly longer doubling time of ~210 min (Figure 3A). To explain the slow-growth phenotypes of the modified clones we entertained three hypotheses, which are neither exhaustive nor mutually exclusive. First, cleavage by Cas9 resulted in a broken chromosome XII, which delayed cell division. The failure to detect wild-type PCR product or bubbles on 2D gels would be explained by this persistent cleavage. Second, Cas9 cleavage resulted in a large-scale reduction of the rDNA copy number as excised rDNA repeats were unable to replicate or segregate efficiently, and were eventually lost by the cells. The reduction in rDNA template would compromise ribosome production and result in slow growth. Third, without functional origins of replication, the completion of chromosome XII replication was delayed as a fork from the adjoining, upstream unique origin would have to traverse the entire rDNA locus. The extension in S phase would delay the cell cycle.

To assess the possible causes of the slower growth, we analyzed whole chromosomes from the transformants by CHEF gel electrophoresis using conditions that allowed us to focus on chromosome XII and the rDNA locus. We looked for broken chromosome XII, extrachromosomal rDNA fragments, or delayed replication of chromosome XII as evidenced by a failure of chromosome XII to enter the gel. In the ethidium bromide stain of the CHEF gels (Figure 2A; compare with Figure S5A), all 16 of the slow-growing clones appeared to be missing their largest chromosome (chromosome XII). However, hybridization of the Southern blot with the proximal (*CEN12*) and distal (*MAS1*) probes (Figure 1A) indicated that each of these slow-growing strains had a shortened version of chromosome XII that comigrated with chromosomes VII and XV (~1090 kb; Figure 2B; compare to Figure S5, B and C). Longer exposures revealed two different subchromosome XII fragments that were consistent with the size of the two chromosome halves if cleavage within the rDNA were occurring (~460 kb for the *CEN12* chromosome arm and ~600 kb for the distal arm containing *MAS1*; the two fragments represent ~5% of the chromosome XII signal) (Figure 2, C and D). To determine whether additional rDNA repeats had integrated elsewhere in the genome or were persisting as extrachromosomal molecules, we reprobed the blots with an *NTS2* rDNA probe (Figure S6). We did not detect free rDNA repeats nor repeats that were housed on other chromosomes. We also did not detect disproportionate hybridization of rDNA to the wells of the slow-growing clones, indicating that chromosome XII from these stationary-phase samples had completed replication.

Because it seemed unlikely that the 5% of cells with a broken chromosome XII could account for the roughly 2.3-fold increase in doubling time, we turned to the hypothesis that the reduction in rDNA copy number (hypothesis #2 above) was

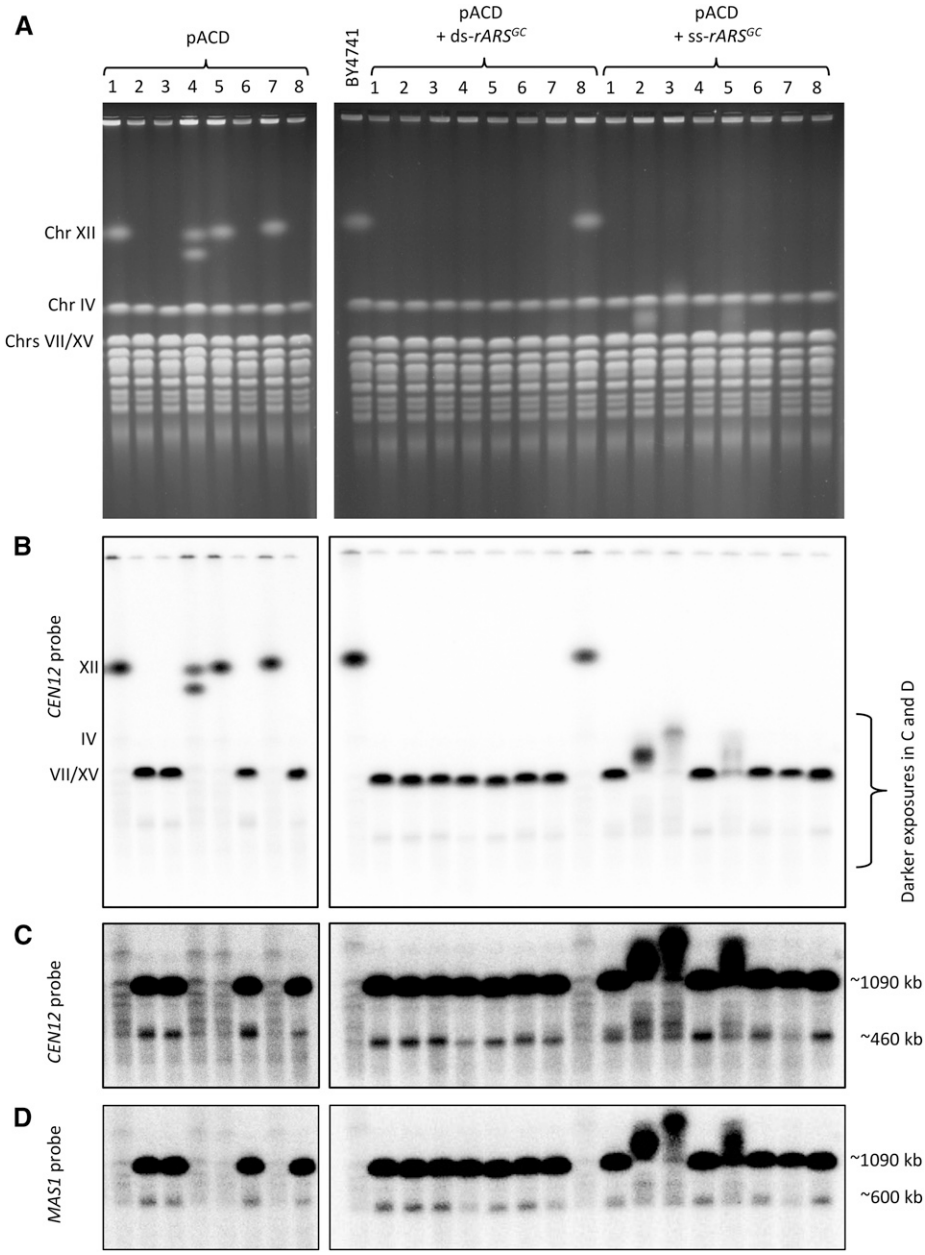


**Figure 2** CHEF gels analysis of CRISPR/Cas9 transformants. (A) The ethidium bromide-stained CHEF gels, run under conditions that maximize the separation of Chr XII, are shown for the same three sets of eight strains shown in Figure S2. (B) Southern blots of the CHEF gels were probed with a fragment from the centromere region of Chr XII. The small Chr XII present in the majority of samples is comigrating with Chrs VII and XV. (C) A longer exposure of the bracketed section of the blots shown in (B) reveals a subchromosomal fragment of ~450 kb. (D) The blots were stripped and reprobed with *MAS1*, which lies on the distal side of the rDNA. A subfragment of ~600 kb is found among the same transformants that had the ~450-kb fragment. Chr, chromosome; CRISPR, clustered regularly interspaced short palindromic repeats; rDNA, ribosomal DNA.

the chief cause of slow growth. Since unique sequences make up ~1060 kb of chromosome XII, the number of rDNA repeats following CRISPR/Cas9 editing could be as low as three or four, although the resolution using these running conditions is not adequate to get an accurate estimate of rDNA length. The CHEF gel of the rDNA$^{\text{“wt”}}$ strains demonstrates that they also have a reduced rDNA copy number (Figure S7A). To estimate the rDNA copy number of the rARS$^{\text{“wt”}}$ and rARS$^{\Delta}$ clones, we digested genomic DNA in gel plugs with *Fsp*I to release the entire rDNA locus as a single restriction fragment (Figure 1A). Using the wild-type chromosomes as size references, we estimate that the three *rARS*$^{\text{“wt”}}$ clones have between 25 and 75 repeats, each clone having broad distributions of ± 10 repeats (Figure S7B). The set of uncharacterized deletion strains from this transformation have in the range of 6–11 rDNA copies, a similar value to that of rARS$^{GC}$-1 and rARS$^{\Delta}$-1.

We suspected that the slow growth of rARS$^{GC}$-1 and rARS$^{\Delta}$-1 was the result of reduced rRNA production since these strains had just nine copies of the rDNA repeats. To measure the relative rRNA content in rARS$^{GC}$-1, we quantified the amount of 25S ribosomal RNA relative to the DNA of a single-copy nuclear gene (*ACT1*) and found a 35% reduction in 25S rRNA in rARS$^{GC}$-1 relative to the parent strain BY4741 (Figure S8), a level of rRNA that is similar to an *orc4* mutant strain with ~10 rDNA copies that arose from a lack of initiation in the rDNA repeats (Sanchez *et al.* 2017). We conclude that hypothesis #2 most-easily explains the slow growth of the edited rDNA strains: Cas9 cleavage releases most of the rDNA repeats from chromosome XII and these repeats are

subsequently lost from the cell. This situation leads to a drastically reduced chromosome XII size and rDNA repeat copy number, which compromises rRNA production, resulting in slowed growth. Crossing rARS$^{GC}$-1 or rARS$^{\Delta}$-1 to BY4742—a wild-type strain with an unedited rDNA array—alleviated the slow-growth phenotype, suggesting that the wild-type chromosome with its ~150 rDNA repeats was meeting the demand for ribosomes. However, in the heterozygous diploids, the mutant rDNA locus further contracted to around two-to-five copies (Figure S7C), suggesting that replication delay of the large origin-free, ~10-copy mutant rDNA locus also may have contributed to the slow growth of the haploids.

### *Reexpansion of the rDNA locus after origin replacement*

We estimate that transformants had grown for 40–45 generations by the time we could examine the size of chromosome XII on CHEF gels or examine replication intermediates on 2D gels. Yet, at a similar number of generations, the transformants with different repair templates had achieved different rDNA repeat sizes (Figure 1B and Figure S7B). To determine whether the differences in chromosome XII sizes and initiation efficiency among the *rARS*$^{\text{"wt"}}$, *rARS1*$^{max}$, and *rARS*$^{GC}$ or *rARS*$^{\Delta}$ strains were due to differences in amplification rates for the edited repeats, we carried out long-term growth experiments using one or more of three different culturing methods: daily serial passaging to keep the cultures in log-phase growth, daily dilution of 1:1000 letting the cells reach stationary phase each day, or continuous culture in a turbidostat where the OD was held constant. For both the *rARS*$^{\text{"wt"}}$ and *rARS1*$^{max}$ strains (passaged daily after reaching stationary phase), we found an initial rapid increase in rDNA copy number followed by a steady, modest increase in chromosome XII of around two repeats per 10 generations of growth that failed to reach the size of the original copy number of ~150 rDNA copies after an additional ~100 generations (Figure S9, A and B).

We examined strains rARS$^{GC}$-1 and rARS$^{\Delta}$-1, which we kept in log-phase growth over a period of 13 days, monitoring OD daily to assess growth rates. The cumulative ODs of two individual colonies of rARS$^{GC}$-1 and three colonies of rARS$^{\Delta}$-1 (Figure 3, A and B) show a striking difference: ~50 generations (160 hr; dotted line Figure 3A) into the experiment, both colonies of rARS$^{GC}$-1 began growing more rapidly and continued growing at the increased rate for the remainder of the experiment. In contrast, rARS$^{\Delta}$-1 colonies did not show this striking change in growth properties. Furthermore, rARS$^{GC}$-1 clones began to show signs of chromosome XII expansion at the same time that the cultures began growing faster (Figure 3C): at ~50 generations the cells were heterogeneous with a majority of the chromosomes remaining at the initial size of ~10 repeats, but by the end of the experiment all cells had expanded their rDNA loci to a median copy number of ~25 repeats. We saw no increase in the size of chromosome XII in the three clones of rARS$^{\Delta}$-1 (Figure 3D).

We repeated long-term growth of *rARS*$^{GC}$ and *rARS*$^{\Delta}$ strains using turbidostats. These continuous culture devices detect when faster growing variants sweep the population because they trigger an increase in the delivery of medium to cultures in an attempt to maintain a constant culture OD. We analyzed five clones of *rARS*$^{GC}$ and three clones of *rARS*$^{\Delta}$ in turbidostats for a period of ~7–8 days (or 85–100 generations). For all but one of them, we found evidence for increased growth rates by the end of the experiment, some more modest than others (Figure 3E and Figure S10A). We collected samples once each day and prepared genomic DNA for CHEF gels (Figure 3F and Figure S10, B and C). By the end of the experiments, we found increases in rDNA copy number for the *rARS*$^{GC}$ cultures but severely restricted amplification in the *rARS*$^{\Delta}$ cultures, findings consistent with the logarithmic, serial transfer experiments.

### *Return of replication initiation to the rDNA NTS2 region of rARS*$^{GC}$ *clones during rDNA expansion*

We isolated single clones from day-10 batch cultures of both rARS$^{GC}$-1a and -1b (Figure 3A) to reanalyze rDNA origin firing after ~100 generations in continuous log phase. The 2D gel analyses of both clones showed low-level initiation within the *NTS2* region, and quantification of the spots corresponding to the 22.4- and 4.5-kb linear fragments confirmed the expansion of rDNA copy number (Figure 4A). We entertained three possibilities to explain the return of origin activity to the rDNA *NTS2* region that was allowing the reexpansion in repeat number beyond the ~10–13 copy ceiling. First, that the initial clone had retained a single wild-type copy of the *rARS* and that, over continuous selection for rapid growth, cells had used this single copy to convert the *rARS*$^{GC}$ mutation back to the wild-type sequence. Second, that other sequences in the *NTS2* had mutated to create a new *rARS*. Third, that a mutation arose elsewhere in the genome in a gene whose altered product was able to recognize *rARS*$^{GC}$ or some other sequence in NTS2. However, as described below, we found no evidence for any of these hypotheses.

To look for return of the wild-type rARS sequence, we PCR amplified and Sanger sequenced a ~600-bp fragment containing the edited regions. We found that the sequences from the faster-growing clones were identical to the initial edited sequence: the *rARS*$^{GC}$ replacement and PAM mutations were still present, and there was no trace of the original wild-type sequence (Figure S3).

To look for origin activity in the flanking regions, we PCR amplified the entire *NTS2* region, cloned it into a nonreplicating plasmid, and checked the library of plasmids for any that were able to replicate autonomously in yeast. The few transformants we recovered had all integrated the selectable marker into the genome, indicating that there were no *NTS2* regions that had acquired a new origin capable of maintaining a plasmid.

To test the hypothesis that a *trans*-acting mutation elsewhere in the genome was recognizing the altered *rARS*, we used a clone from day 10 of the evolution as a host in a transformation experiment in which we introduced the

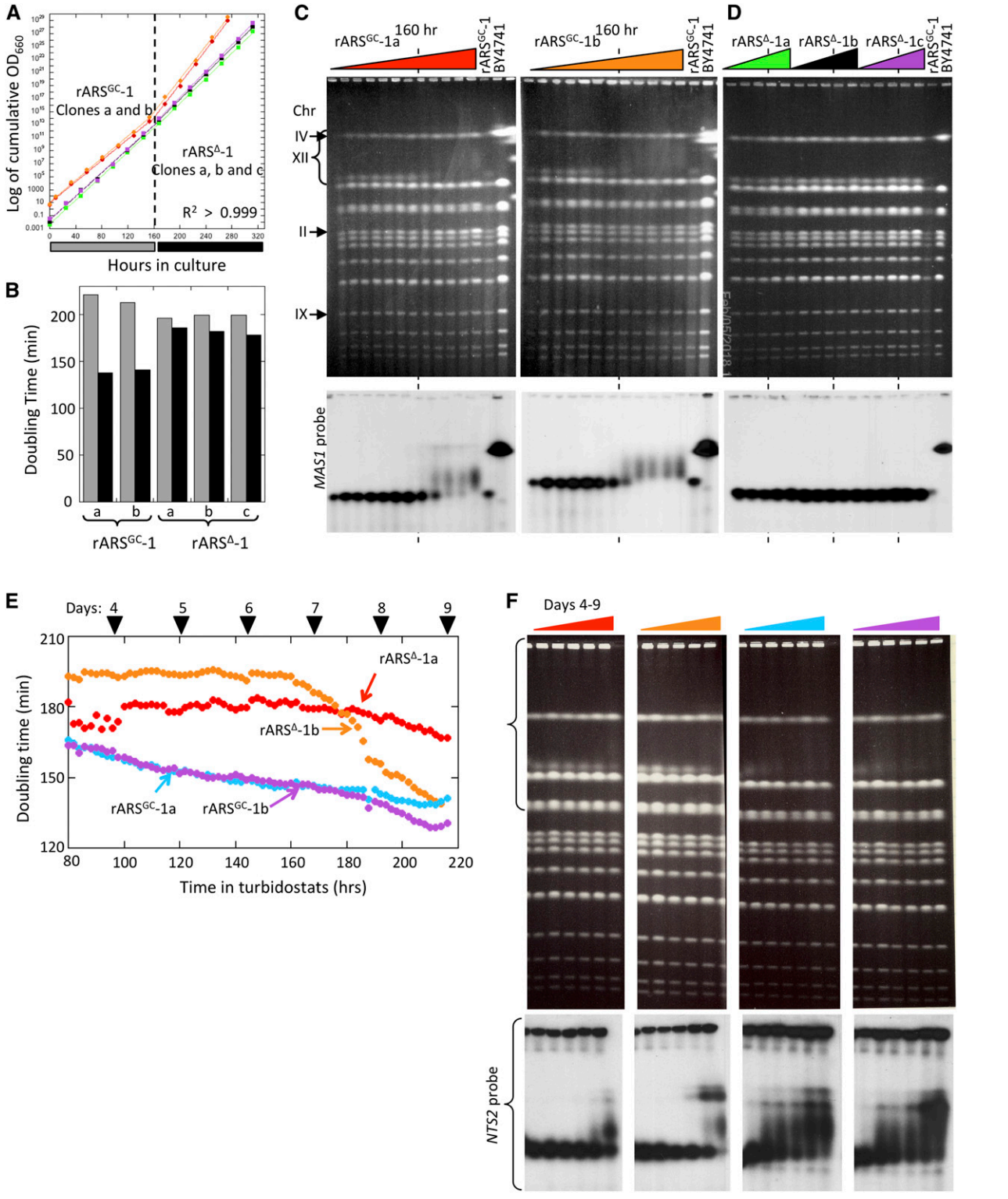


**Figure 3** Monitoring changes to growth rates and Chr XII size during extended growth of rARS$^{GC}$-1 and rARS$^{\Delta}$-1. (A) Cumulative OD for cultures kept in continuous logarithmic growth. Two clones of rARS$^{GC}$-1 (-1a and -1b) and three clones of rARS$^{\Delta}$-1 (-1a, -1b, and -1c) were followed for ~13 days. (B) Population doubling times for the first (gray) and second (black) halves of the continuous growth experiments in (A). (C and D) CHEF gel analysis of the changes to Chr XII size over ~13 days: gels in (C) contain samples collected each day, gels in (D) contain samples collected on days 0, 3, 6, 9, and 12. The conditions for CHEF gel electrophoresis allow the detection of subtle changes in Chr XII size. Only the top halves of the Southern blots probed with *MAS1* are shown. (E) Growth rates for *rARS$^{GC}$* and *rARS$^{\Delta}$* clones in turbidostats. The growth rates over the last ~6 days of the turbidostat runs are shown. (F) CHEF gels for samples harvested on days 4 through 5 are shown. The Southern blots were probed with the *NTS2* probe and reveal changes in Chr XII/rDNA over the course of the continuous growth. ARS, autonomous replication sequence; Chr, chromosome.

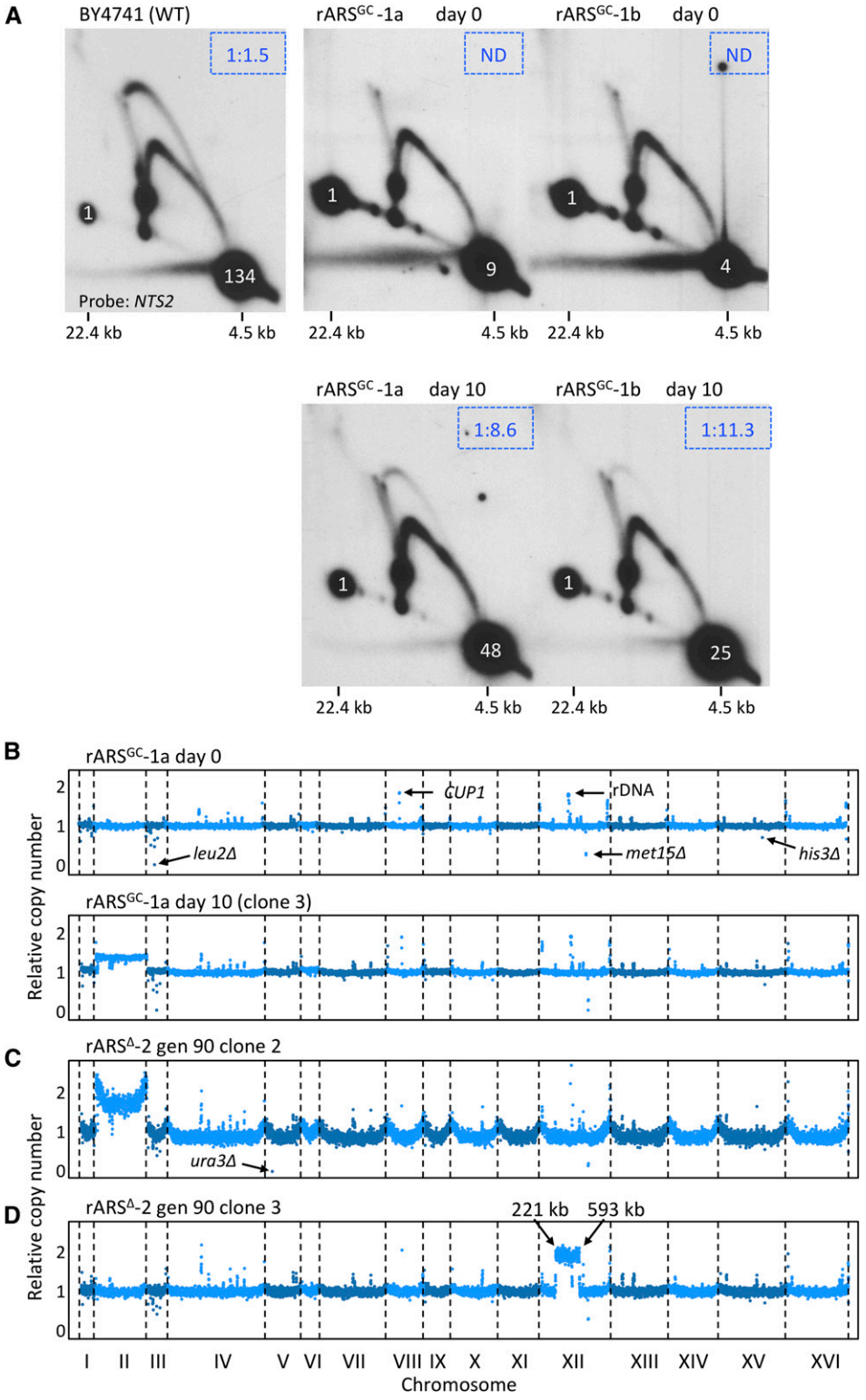


**Figure 4** WGS and 2D gel analysis of *rARS*$^{GC}$ and *rARS*$^{GC}$ isolates, at day 0 and day 10 of the continuous growth experiments. (A) The Southern blots of 2D gels were probed with the *NTS2* probe to assess origin function. rDNA copy number estimates (in white type) are deduced from the relative signal of the 4.5-kb fragment to the 22.4-kb junction fragment. The BY4741 and rARS$^{GC}$-1a day-0 gels are the same as in Figure 1B. The day-10 samples are from clones isolated from the day-10 populations. (B) Read-depth analysis from WGS for the rARS$^{GC}$-1a samples shown in (A). Read-depth measurements across 1-kb bins were normalized to the genome average. Individual values below ~1.0 are seen for the various auxotrophic deletions in the parent strain BY4741 (*leu2*Δ, *ura3*Δ, *met15*Δ, and *his3*Δ). Individual values > 1.0 indicate multiple mapping of Ty transposable elements, the repeated *CUP1* locus on chr VIII, and the rDNA locus on chr XII. In this clone from day 10, one-half of the cells appear to be disomic for chr II. (C and D) WGS read-depth analysis for two clones of rARS$^{\Delta}$-2 isolated on day 9 (90 generations) of the continuously passaged culture. Clone 2 is disomic for chr II (the increased copy number of sequences near telomeres is an artifact of the library preparation). Clone 3 has a segmental aneusomy for a region of chr XII between two directly repeated Ty long terminal repeats at positions 221 and 593 kb. 2D, two-dimensional; ARS, autonomous replication sequence; chr, chromosome; ND, no signal above background was measured; rDNA, ribosomal DNA; WGS, whole-genome sequencing.

*rARS*$^{GC}$ plasmid library (see above). Again, we recovered no transformants that were able to support replication of the *rARS*$^{GC}$ plasmid library members as free plasmids, arguing against the possibility that a second site mutation was allowing initiation within the edited rDNA. However, it remains possible that this result using plasmid transformation may not be capturing unique chromatin/chromosome architecture in the rDNA locus.

From these combined results, we have no direct result supporting a genetic cause for the return of initiation to the rDNA *NTS2* region. Yet, the striking difference in rDNA expansion between the rARS$^{GC}$-1a and -1b clones, and the

rARS$^{\Delta}$-1a, -1b, and -1c clones, suggested that the sequence of the *NTS2* region was somehow important for the amplification of the rDNA and for the generation of faster-growing suppressors. To test this conclusion further, we sequenced the genomic DNA from day-10 populations, and clones of the rARS$^{GC}$-1a and -1b growth experiments. In comparison to the day-0 clones of these two cultures, there were no alterations to the rDNA repeats and no SNPs in genes relevant to DNA replication (Table S2). However, it was notable that rARS$^{GC}$-1 had indels in *IRA1* or *IRA2*, which may have been important for enhancing the growth and the subsequent improved fitness of the evolved strains derived from this background (Colombo *et al.* 2004).

### *Chromosome aneuploidy contributes to improved growth of rARS$^{GC}$ and rARS$^{\Delta}$ strains*

The lack of any single-nucleotide variants that could explain improved growth rates led us to investigate large-scale changes by using the WGS data to investigate copy number differences across the genome. Read-depth analysis of the WGS of the day-10 clone of rARS$^{GC}$-1a from the serial passaging experiment (Figure 3A) suggested that the cells had become disomic for chromosome II (Figure 4B). Consistent with this idea, the ethidium bromide photograph of the CHEF gel for rARS$^{GC}$-1 (Figure 3C) suggested that by the end of the experiment, the intensity of the chromosome II signal was elevated relative to that of the surrounding chromosomes. Comparative hybridization with probes from the centromere-adjacent regions of chromosomes II and IX confirmed the chromosome II disomy for rARS$^{GC}$-1a (Figure S11). The CHEF gel of the three *rARS*$^{\Delta}$ evolutions (Figure 3D) indicated that in two of them (rARS$^{\Delta}$-1b and -1c) there had also been an amplification of chromosome II.

As it appeared that chromosome II aneuploidy was a recurring event that we detected following the reduction in rDNA replication initiation or copy number, we examined the serial passaging experiments with the independent isolates of *rARS$^{GC}$* and *rARS*$^{\Delta}$ (clones rARS$^{GC}$-2 and rARS$^{\Delta}$-2). We found comparable results for rDNA amplification: there was no significant amplification of the rDNA locus in rARS$^{\Delta}$-2 but slight amplification in rARS$^{GC}$-2 (Figure S12, A and B). From these two experiments, we isolated four individual clones at generation 90 for further analysis (Figure S12A). We compared Cen2/Cen9 hybridization to track and quantify the appearance of the chromosome II disome over time (Figure S12, C–E). The population of rARS$^{GC}$-2 was essentially homogeneous for chromosome II disomy by generation 50 and all four clones from day 9 of the passaging experiments were disomic for chromosome II. No significant increase in chromosome II was detected in the population during passaging of rARS$^{\Delta}$-2; however, clone#2 from generation 90 contained an additional copy of chromosome II (Figure S12E).

To determine whether disomy for chromosome II actually provides a selective advantage for the strains with reduced rDNA copies, we crossed clone 1 from the rARS$^{GC}$-2 passaging experiments (Figure S12, A and E) with BY4742, and examined the growth properties of segregants containing the parental and derived chromosome XIIs, with and without an extra copy of chromosome II (Figure 5A). We examined six complete tetrads for their patterns of chromosome segregation and analyzed the growth properties for the spores of four of these tetrads (Figure 5, B and C). The presence of an extra copy of chromosome II improved the growth of the strains that contained *rARS$^{GC}$* by nearly 30 min (~16% improvement in doubling time), but increased the doubling time by 8 min (~10%) in strains with the wild-type rDNA origin and intact rDNA array.

We performed WGS for the four generation-90 clones from rARS$^{\Delta}$-2 (Figure S12A). Read-depth analysis confirmed the chromosome II disomy of clone 2 and revealed a different aneuploidy for clone 3 (Figure 4, C and D). In this clone, a region of chromosome XII of ~370 kb, from coordinate 221 kb (YLRWδ 4) to 593 kb (YLRWδ10), was present in two copies. Between these two LTRs lie the rDNA locus, and both *MAS1* and *CDC45*. This duplicated segment is located on chromosome XII and, along with ~10 copies of the rDNA repeats, accounts for the increased size of chromosome XII seen on the CHEF gel (clone #3; Figure S12C). The ratio of *MAS1* or *CDC45* to *CEN9* supports our conclusion that an intrachromosomal duplication between two LTRs has allowed the total copy number of rDNA repeats to double in this particular clone, without expanding either rDNA locus beyond the apparent limit of ~10 ARS-less repeats. Although we were unable to find a clone with this chromosome XII duplication from either of the rARS$^{GC}$-1 passaging experiments, we did see the transient appearance of this larger chromosome XII during the later days of the rARS$^{GC}$-1a passaging experiment (Figure 3C) and in many of the turbidostat cultures (Figure 3F and Figure S10C). We also sequenced the population samples from the last day of each of the eight turbidostat cultures (Figure 4E, Figures S10 and S13, and Tables S2 and S4). For all eight of the cultures, we found chromosome aneuploidies/aneusomies that accumulate to different extents in the populations: five cases of chromosome IV disomy, two cases of chromosome XII disomy, and one case of an internal duplication of the rDNA locus on chromosome XII (Figure S13 and Table S4). For none of the populations did we find common single-nucleotide variants that could easily explain the entirety of the improved growth rates (Table S2).

### *The effect of rDNA origin replacement on ERCs and rDNA reexpansion*

Using the hygromycin system of rDNA manipulation, Ganley *et al.* (2009) introduced two different versions of the *ARS1* origin, along with a selectable *URA3* marker, into the yeast rDNA locus that had been reduced to two copies. They found that the efficiency of the rDNA origin influences both the production of ERCs and the rate at which the rDNA locus reexpands. ERCs are thought to be formed primarily through homologous recombination between adjacent or nearby rDNA repeat units, which results in the excision of a circular

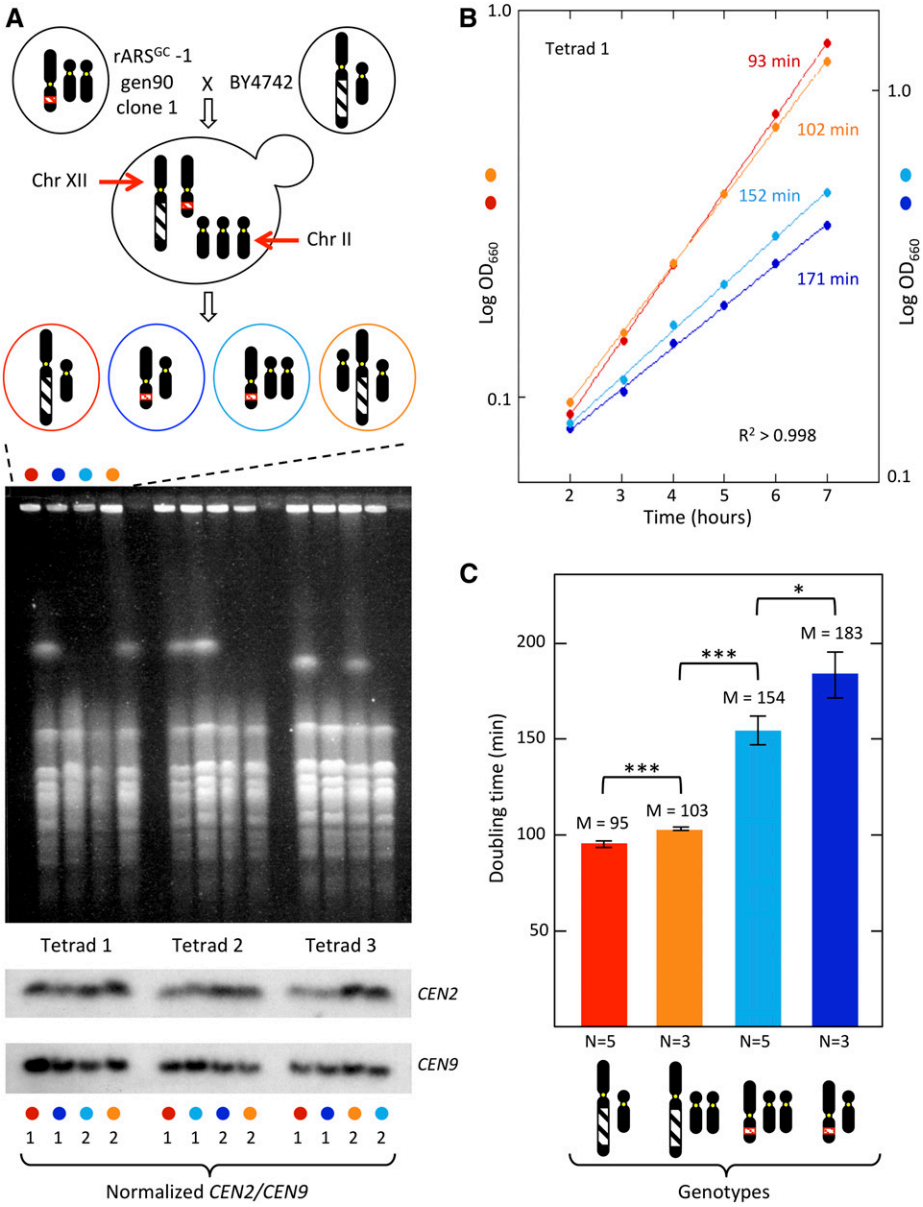


**Figure 5** Scheme for analyzing the growth properties of Chr II disomy in strains with the native rDNA and with *rARS*$^{GC}$. (A) Top: the scheme for mating clone 1 from generation 90 of the rARS$^{GC}$-2 serial passage experiment (Figure S12A) with BY4742 and segregation to form a tetra-type tetrad. Middle: ethidium bromide-stained CHEF gel of three tetra-type tetrads from the cross. Bottom: Southern blots to follow segregation of Chr II disome. (B) Growth rates for the four spores from tetrad 1 in part (A). (C) Average growth rates for similar genotypes isolated from four independent tetrads. Significance values were calculated using the Student's *t*-test: * $P < 0.05$ and *** $P < 0.005$. ARS, autonomous replication sequence; Chr, chromosome; rDNA, ribosomal DNA.

DNA molecule containing one or more complete rDNA units. ERCs are capable of self-replication based on the strength of the *rARS* and are asymmetrically retained in the mother cell, causing them to increase dramatically in copy number with mother cell age (Sinclair and Guarente 1997). To compare the two methods of altering the rDNA origin, we analyzed our *rARS*-modified strains for the presence of ERCs.

We anticipated finding differences in the steady-state levels of ERCs among the edited strains, as the efficiency of the rDNA origin should affect their ability to propagate ERCs. For example, the *rARS*$^{\Delta}$ strains might be able to produce ERCs by intramolecular recombination, but once formed they would not be able to initiate replication and would be diluted at cell division. To assess the relative ERC populations among different edited strains, we analyzed portions of freshly prepared plugs using conventional gel electrophoresis. Under these conditions, all of the yeast chromosomes run at limiting mobility with different circular multimers/topological forms running both above and below this band (Figure 6A). By comparing the hybridization signals of the two lowest circular forms to that of the chromosomal rDNA band, we found that the steady-state level of ERCs in these predominantly young cell populations was proportional to the potential efficiency of the different rDNA origins, with the *rARS1*$^{max}$ transformants maintaining > 100 times higher levels of ERCs than BY4741. At the other extreme, we were unable to detect ERCs in either the *rARS1*$^{GC}$ or *rARS*$^{\Delta}$ strains.

The high levels of ERCs in the *rARS1* and *rARS1*$^{max}$ strains prompted us to look more carefully at the initial transformants of both *rARS1* and *rARS1*$^{max}$ (samples at ~45 generations; Figure S14, A and B). Of the clones that had successfully replaced the *rARS*, there were five clones that

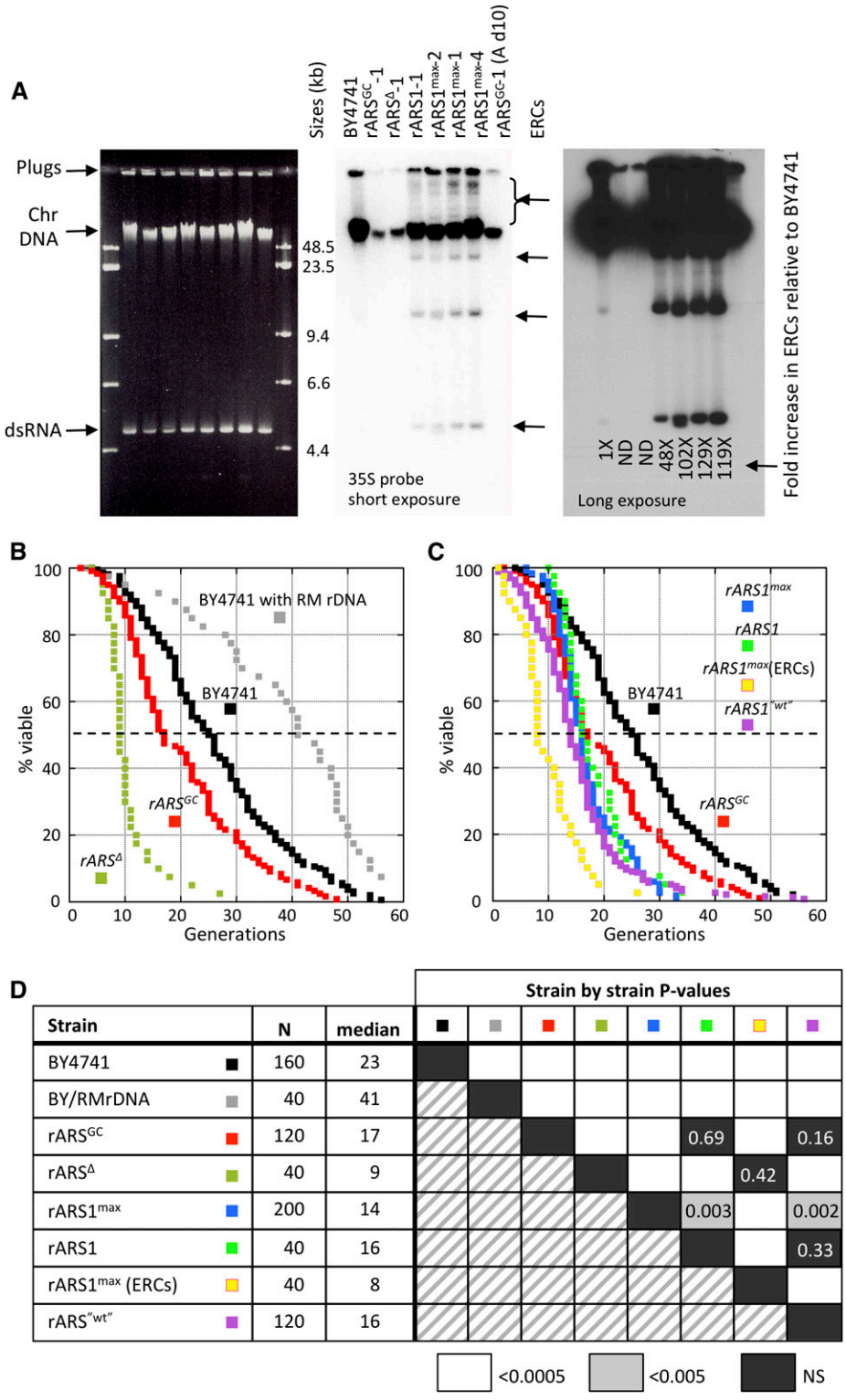


| Strain | N | median | | | | | | | |
|---|---|---|---|---|---|---|---|---|---|
| BY4741 | 160 | 23 | | | | | | | |
| BY/RMrDNA | 40 | 41 | | | | | | | |
| rARS$^{GC}$ | 120 | 17 | | | | | 0.69 | | 0.16 |
| rARS$^{\Delta}$ | 40 | 9 | | | | | | 0.42 | |
| rARS1$^{max}$ | 200 | 14 | | | | | 0.003 | | 0.002 |
| rARS1 | 40 | 16 | | | | | | | 0.33 |
| rARS1$^{max}$ (ERCs) | 40 | 8 | | | | | | | |
| rARS$^{"wt"}$ | 120 | 16 | | | | | | | |

**Figure 6** ERC frequency and consequences for replicative life span among the different *rARS* replacement strains. (A) DNA prepared in agarose plugs was run on a standard 0.5% agarose gel where chromosomes and circular molecules are easily distinguished. The Southern blot using a probe from the 35S gene is shown at two exposure levels. The ratio of hybridization to the two lower bands was quantified and compared to the signal from the chromosomal band. That ratio in BY4741 was defined as 1 and other strains were normalized to that value. (B) Life span curves for the strains that were transformed with either *rARS*$^{GC}$ or *rARS*$^{\Delta}$ are compared with BY4741, and the long-lived BY strain with the rDNA from RM11-1A. (C) Life span curves for strains transformed with functional ARSs are compared with BY4741 and the long-lived BY strain with the rDNA from RM11-1A. Multiple independent transformants were separately examined, and the data pooled to generate the life span curves for *rARS1*$^{max}$ and *rARS*$^{"wt"}$. The life span curves for *rARS1* and *rARS1*$^{max}$ (ERCs) were generated from single transformants. The BY4741 and *rARS*$^{GC}$ data are reproduced from (B). (D) The number of mother cells followed (*N*) and the median life spans were determined for each class of mutant. *P*-values from the Wilcoxon rank-sum analyses for each pairwise strain comparison are shown. Highly significant values ($P < 0.0005$) are indicated by white squares; NS values are indicated by black squares. ARS, autonomous replication sequence; Chr, chromosome; ERC, extrachromosomal rDNA circle; NS, nonsignificant; rDNA, ribosomal DNA.

had an even smaller chromosome XII than the rARS$^{GC}$-1 parent clone (*rARS1*$^{max}$ clones 2, 4, and 7, and *rARS1* clones 2 and 5; *MAS1* probe in Figure S14, A and B). On reprobing the blots with the 35S probe, we found that these clones showed little to no hybridization to chromosome XII, but additional rDNA-positive bands appeared at positions where no corresponding chromosomes were present (horizontal arrows; Figure S14, A and B). These bands are consistent with the properties of circular molecules of different sizes (monomers and dimers, *etc*.) and topologies (supercoils and nicked circles) (Brewer *et al.* 2015). The suggestion that no *NTS2* sequences exist on chromosome XII is corroborated by the 2D

gel analysis of *Nhe*I-digested genomic DNA that we performed on two of the clones: the *NTS2* probe no longer detected the 22.4-kb junction fragment between rDNA and the distal arm of chromosome XII (Figure S14C). This extrachromosomal state of the rDNA is clonally stable on solid culture medium: we restreaked individual clones from the rARS1$^{max}$-4 transformant and found, ~30 generations later, that each clone retained high levels of ERCs (Figure S15A). However, upon serial passaging of rARS1$^{max}$-4 in liquid medium, the ERCs largely disappeared by 30 generations and chromosome XII again contained rDNA repeats (Figure S15B). Over the remaining ~100 generations the rDNA slowly expanded, but at a much slower rate than we observed for rARS1$^{max}$-8 (compare Figure S15B with Figure S9B and Table S4).

### *The consequence of rDNA origin replacement for replicative life span*

A variety of observations in yeast and other eukaryotes have shown that the rDNA plays a significant role in determining replicative life span, which is defined as the number of daughter cells produced by a mother cell prior to irreversible cell cycle arrest (Mortimer and Johnston 1959). First, an *rARS* ACS variant found in the vineyard strain RM11-1A reduced the efficiency of the rDNA origin and extended life span (Kwan *et al.* 2013). Second, a reduction in total ribosome levels through calorie restriction, chemical interventions such as rapamycin, or genetic manipulations through the deletion of ribosomal subunit proteins (Lin *et al.* 2000; Kaeberlein *et al.* 2005; Chiocchetti *et al.* 2007; He *et al.* 2018) all robustly extend life span across the evolutionary tree. Third, in yeast, the accumulation of ERCs in mother cells has been linked to life span (Sinclair and Guarente 1997). Deletion of Fob1, a protein that binds to the RFB site in each rDNA repeat, and blocks head-on collisions between RNA Pol1 and the replication complex, reduces ERC levels and dramatically extends life span (Defossez *et al.* 1999). As our edited rDNA strains have variations in their rDNA origins, significantly reduced rDNA copy number, reduced ribosomal RNA content (Figure S8), and variable levels of ERCs, we decided to conduct replicative life span analysis on representatives of the different origin replacement strains that we generated.

We micromanipulated individual, newly "born" daughter cells on agar plates. We monitored the cells, counting and removing consecutive daughter cells. BY4741 and the BY4741 strain with the rDNA locus from RM11-1A (Kwan *et al.* 2013) were used as the normal (mean life span = 23 generations) and long-lived (mean life span = 41) controls, respectively. We anticipated that *rARS$^{GC}$* and *rARS$^{\Delta}$* strains, with severely restricted origin activity in the rDNA, would have extended life spans. Contrary to our expectations, we found reduced life spans for both strains (Figure 6, B and D), with *rARS$^{\Delta}$* having a median life span of only nine generations. Life spans for the chromosomally integrated *rARS1* and *rARS1$^{max}$* strains were similar to those of the *rARS$^{GC}$* variants (Figure 6, C and D). Perhaps most surprising were the similar life spans of the *rARS1$^{max}$* variant that has only ERCs (rARS1$^{max}$-4) and the *rARS$^{\Delta}$* strain that has no ERCs (Figure 6, B and C). Unfortunately we cannot currently measure either the rDNA copy number or the level of ERCs for the individual mother cells that were analyzed for life span. However, if these mother cells accurately represent the cultures from which they were isolated, then our data suggest that drastically reduced rDNA copy number masks any benefit to life span that may result from rDNA origin status or ERC levels.

## Discussion

CRISPR/Cas9 and its many offshoots have been successfully used for editing of an enormous variety of genetic targets in many organisms. Targets have been almost exclusively single copy and worries about off-target cutting have been prominent concerns. In this work, we have set out to ask: can we edit tandem repeats, how efficiently, and at what phenotypic costs? We have worked out conditions for targeting the ~150 identical origins in the rDNA locus simultaneously, how to repair the breaks with templates of our choosing, and to follow the phenotypic consequences of the modified homogeneous rDNA arrays. From our WGS analysis, we find no obvious off-target edits (Table S2).

The rDNA locus in most organisms is difficult to genetically modify through more conventional techniques such as random mutagenesis or even targeted gene-replacement strategies that require selectable markers, because of the seemingly impossible task of altering every member of the array. Yet, an ever-growing list of biological processes, in addition to ribosome biogenesis, are linked to the rDNA and the nucleolus that forms around the rDNA (Boisvert *et al.* 2007; Bahadori *et al.* 2018). Recently, rDNA copy numbers in several cancers have been found to be lower than in matched noncancerous biopsies (Wang and Lemos 2017; Xu *et al.* 2017) and appear to be increased in some patients with schizophrenia (Chestkov *et al.* 2018). However, at this point the causality of rDNA changes in these diseases is undetermined. In addition, variation in nucleolar size has been shown to correlate with life span (Tiku *et al.* 2017). In experimental organisms, sequence variations in the noncoding regions of the rDNA have been documented but again their significance is difficult to determine (Ganley and Kobayashi 2007; James *et al.* 2009; Kwan *et al.* 2013). Natural variation in rDNA sequences and copy numbers are found even between closely related strains of yeast (James *et al.* 2009), yet almost nothing is known about how these differences influence any of the disparate functions attributed to the rDNA locus.

We chose to edit the rDNA origin of replication, an ~100-bp region between the divergently transcribed 35S and 5S genes in each repeat of the yeast rDNA array. One of the long-standing mysteries regarding the *rARS* is the observation that while each 9.1-kb repeat contains an identical *rARS* sequence, only a subset of repeats contains an active origin. The general inefficiency of the rARS on plasmids is thought to be due to the

fact that the *rARS* ACS differs from the consensus sequence by a single G within one of the T tracts. An additional SNP is found in the ACS of the vineyard strain, RM11-1A, which reduces its plasmid-maintenance properties even more. These noncanonical ACSs may help to explain the low efficiency of the *rARS* on plasmids; however, in the rDNA locus, transcriptional activity of adjacent rDNA repeats has also been shown to correlate with active origins (Muller *et al.* 2000). Furthermore, it is not known whether this origin inefficiency is a selected property, how it participates in or influences rDNA copy number, or how the status of the *rARS* influences the creation and/or segregation of ERCs that have been associated with replicative aging. To begin addressing these questions, we have successfully replaced the rARS with both potentially more- and less-efficient origins, and have characterized the key phenotypic effects of origin replacement.

To summarize our findings on Cas9 editing of the rDNA replication origin, we find that even with a single single-guide RNA, complete replacement of the rDNA ARS was efficient: when replacing the *rARS* with *ARS1* or $ARS1^{max}$, we found that 8 of 12 colonies and 5 of 12 colonies tested (Figure S4B), respectively, had incorporated the introduced origin within the rDNA repeats. Deleting or introducing a loss-of-function mutation into the *rARS* appears less efficient (1–2 of 16 colonies; Figure S2C), perhaps due in part to viability problems that result from having no functional origin within the rDNA array. Regardless of which repair template we supplied, we found that cells respond to the severe reduction in rDNA copy number that results from Cas9 cleavage in one of three ways. First, transformants that fail to use a template for repair of the break delete the sequences between the most distal PAM sites and are unable to expand their rDNA locus beyond ~10 copies. Long-term growth selects for cells that have acquired an additional copy of chromosome II, IV, or XII, or have duplicated the entire rDNA locus through recombination at distantly located direct repeats (chromosome XII segmental aneusomy). Second, transformants that repair their chromosome XII breaks with the $rARS^{GC}$ template can increase the number of tandem rDNA repeats and show a very modest return of origin activity to the NTS, even though they retain only the GC mutant rARS. However, this level of expansion does not completely restore fitness as cells benefit from either whole-chromosome disomy (chromosome II, IV, or XII) or chromosome XII segmental aneusomy. Third, transformants that have the wild-type rDNA template (or *rARS1* or $rARS1^{max}$) for repair also experience a transient reduction in rDNA copy number. However, they are able to expand their rDNA locus, but within 100–150 generations do not reach the original ~150 repeats.

Based on our observations, using a variety of templates to repair Cas9 breaks in the rDNA, we suggest that the pathway of CRISPR/Cas9 editing is very similar to one proposed by Muscarella and Vogt (1993) for how cells survive cleavage of the rDNA locus by an endogenously expressed I-*Ppo*1 restriction enzyme. This similarity was also recognized by Chiou and Armaleo (2018). I-*Ppo*I cuts once in each rDNA repeat and nowhere else in the *S. cerevisiae* genome (Lowery *et al.* 1992); however, surviving clones with mutations or insertions at the cleavage site are readily obtained. Upon sequencing, all of the repeats within a clone were found to share the same event, yet different clones experienced unique events. Muscarella and Vogt imagined a series of breaks that were repaired off a single mutant template, eventually sweeping through the 150 rDNA copies. While they did not examine rDNA copy number or chromosome XII sizes, it is likely that the I-*Ppo*I survivors also experienced the reduction in rDNA size that we have observed with Cas9 cleavage. In our experiments, we provided repair templates that, once incorporated into the genome, could serve as the template for repair of additional fragmented repeats.

Taking into account the evidence from the different rDNA editing experiments we performed, we suggest the following model for how CRISPR/Cas9 editing leads to a homogeneous rDNA array (Figure 7): The ~20-fold difference in transformation frequency of pML104 and pACD suggests that Cas9 cleaves the PAM sites in the rDNA locus efficiently (Figure 7, items 1 and 2), and that for most cells cleavage is lethal. It is this lethality that allows us to detect repair without the need for a selectable marker. The rare cells that survived pACD transformation with their rDNA intact are likely to be the result of plasmid mutations that create a loss-of-function mutation in Cas9 or loss of the guides. For cells to survive cleavage of the rDNA repeats, they would need to repair the broken chromosome by eliminating the target sites of the guide RNAs. We find that they repair the damaged locus in one of two ways: either the cut ends repair by nearby microhomology-directed recombination (Figure 8 and Figure S3B) or they use the larger homology provided by the template with the altered PAM sites (Figure 7, item 3). The majority of the linear fragments (rDNA fragments and the repair template) are lost through degradation (Figure 7, item 4). After rejoining the two halves of chromosome XII (Figure 7, item 3), it would only take the repair of a single excised repeat—by joining the two ends to form a circular DNA molecule (Figure 7, item 3)—to create a more stable, noncleavable template for the repair of additional repeats, their reintegration into chromosome XII (Figure 7, item 5), and expansion by unequal sister chromatid exchange (Figure 7, item 6). Our results with transformations using *rARS1* and $rARS1^{max}$ templates provide evidence for the rebuilding phase of the model: we found that roughly one-third of the clones had only ERCs and no appreciable *NTS2* sequences remaining on chromosome XII. The one clone that we grew in liquid culture for an additional 170 generations demonstrated a rapid repopulation of the rDNA locus on chromosome XII (Figure S15B), presumably through integration of the ERCs. However, after rebuilding the chromosomal rDNA locus, these strains still maintain much higher steady-state levels of ERCs—~100-fold higher than the wild-type strain—while the strains with either $rARS^{GC}$ or $rARS^{\Delta}$ had no detectable ERCs. The lack of ERCs in strains with either $rARS^{GC}$ or $rARS^{\Delta}$

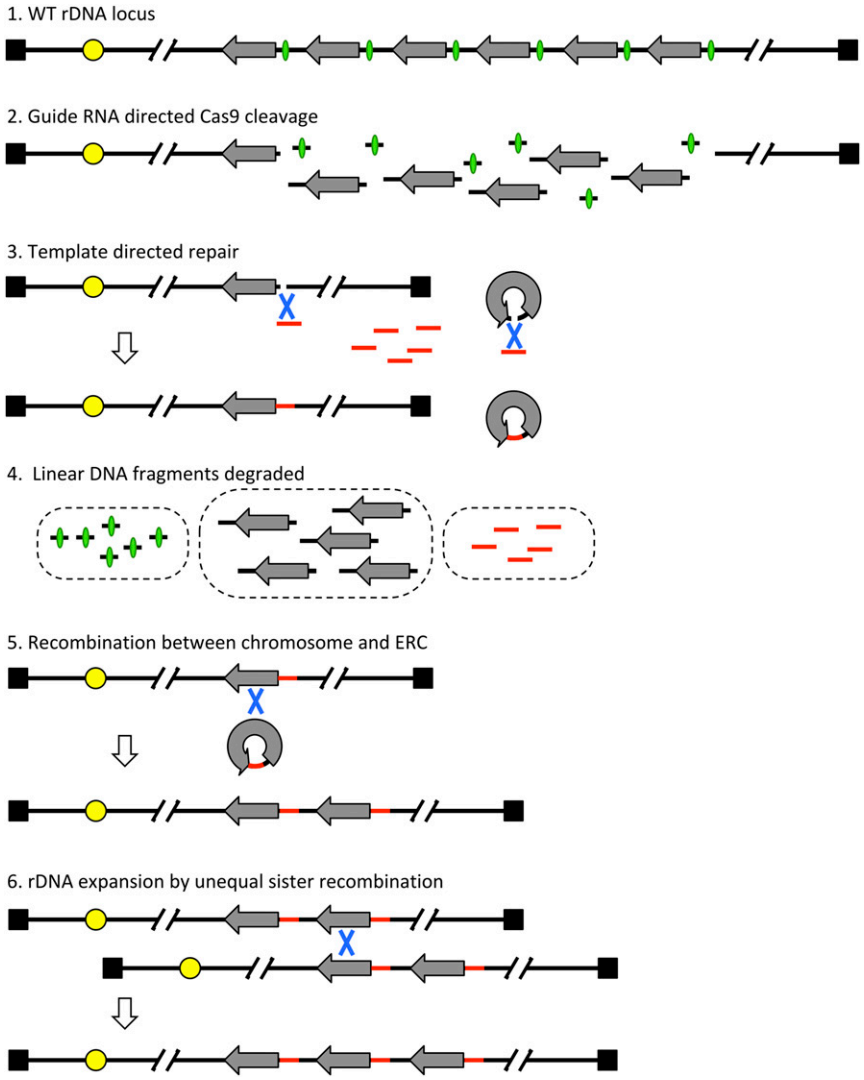


**Figure 7** A proposed mechanism for CRISPR/Cas9 editing of the repeated rDNA locus. The excised rDNA nontranscribed spacer region that includes the origin is indicated by green ovals; the repair templates are indicated by red lines. The centromere of chromosome XII is a yellow circle and the telomeres are black squares. CRISPR, clustered regularly interspaced short palindromic repeats; ERC, extrachromosomal rDNA circle; rDNA, ribosomal DNA.

is likely the consequence of the inability of the ERCs to replicate once they are formed, although we cannot rule out the possibility that the status of the ARS is also playing a role in the ability of the ERCs to be excised from the rDNA locus.

Clones that had been successfully edited came up slowly on transformation plates and retained their slow growth upon restreaking on selective plates, suggesting that they may be compromised in their ability to synthesize rRNA. However, the only clones that maintain this slow growth on prolonged subculturing are those that have deleted *rARS* completely. It appears that the rDNA copy number that these strains are able to stitch back together reaches a maximum at ~10 copies. Limitations on replication are likely the cause of this ceiling. Since the rDNA locus is replicated unidirectionally, in the same direction as transcription, a single fork from the adjacent non-rDNA origin ~30 kb away would be responsible for replicating the entire 90-kb rDNA locus. Nowhere else in the yeast genome are potential origins of replication so distantly spaced (Raghuraman *et al.* 2001; http://cerevisiae.oridb.org). At an average fork speed of ~3 kb/min (Rivin and Fangman 1980), a 120-kb replicon would take longer than the ~30-min S phase to complete replication. But there is reason to suspect that this fork would not be capable of the average speed because of the very high density of slower-moving PolI transcription complexes (Schneider *et al.* 2007) that would be in the way (French *et al.* 2003; Ide *et al.* 2010). We envision two possible consequences of trying to replicate this rDNA locus from an adjacent origin: either the cell cycle would be delayed, or cells would proceed into mitosis with an unfinished chromosome XII and suffer a double-stranded break within the incompletely replicated rDNA locus. At ~45 generations, we see significant (5%) chromosome XII breakage, which could reflect ongoing Cas9 editing or mitotic catastrophe from incomplete replication at the rDNA locus. The broken chromosome XIIs disappear upon continuous subculturing, suggesting that the cells have eventually completed the editing process or have solved the replication delay problem in some other way.

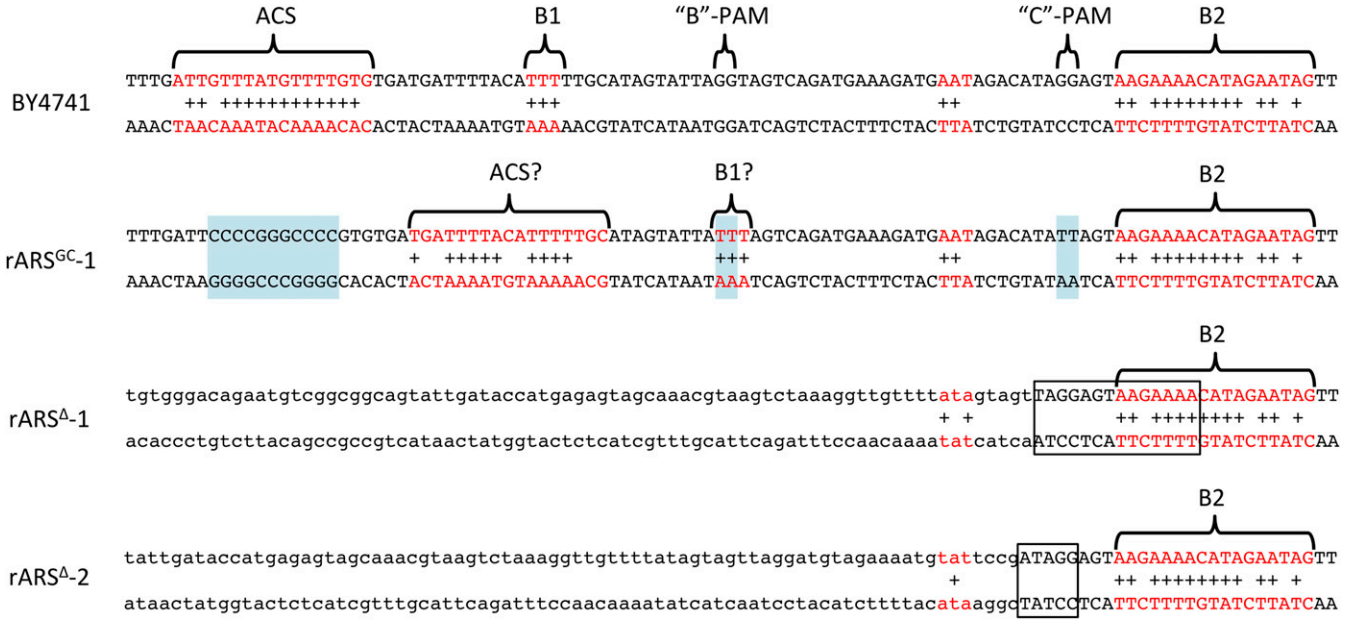


**Figure 8** Identification of a cryptic origin in *rARS*$^{GC}$. The core of the rDNA origin from BY4741 is shown with the ACS, the B1 elements, and the B2 element in red type with a plus sign (+) indicating a match to the consensus sequences. Note, this orientation of sequence is opposite to the orientation in Figure 1A, to conform to the usual orientation of ARS sequences that places the T-rich strand of the ACS on the Watson strand to the left and the B2 element on the right. Blue shaded boxes for rARS$^{GC}$-1 highlight the GC replacement in *rARS*$^{GC}$, and the PAM site mutations associated with guides B and C. The brackets and red type highlight potential alternate ACS and B1 elements in *rARS*$^{GC}$. rARS$^{\Delta}$-1 has a deletion of 167 bp and rARS$^{\Delta}$-2 has a deletion of 144 bp. Each deletion removes all four guide sequences and three of the four PAM sites. The lower-case nucleotides were originally 167- or 144-bp to the left of the junctions, respectively. The boxed sequences indicate the microhomology at the deletion junctions. ACS, ARS consensus sequence; ARS, autonomous replication sequence; PAM, protospacer adjacent motif; rDNA, ribosomal DNA.

We have discovered several advantageous chromosomal amplifications that accompany long-term growth of the *rARS*$^{\Delta}$ and *rARS*$^{GC}$ strains: aneuploidy for chromosome II, chromosome IV, or chromosome XII, and aneusomy for the region of chromosome XII that contains the rDNA locus. While we have not identified how chromosome II or chromosome IV aneuploidy improves fitness for the *rARS*$^{\Delta}$ and *rARS*$^{GC}$ strains, it is likely that some gene or genes on these chromosomes, when present in a second copy, could improve some aspect of DNA replication, protect cell cycle transitions, or increase rRNA synthesis. The potential benefit of chromosome XII aneusomy/aneuploidy is more easily understood. By creating a direct repeat of the rDNA segment of chromosome XII between two directly oriented repeats or by maintaining a second copy of the whole chromosome, the cell doubles its ability to produce rRNAs without exceeding the ~120-kb ceiling on replicon size. Whatever detrimental effects result from having other genes in a second copy (Torres *et al.* 2007), they are countered by the benefit of increased rRNA production.

Unlike clones with *rARS*$^{\Delta}$ that are unable to expand their rDNA copy number past ~10 copies, strains with *rARS*$^{GC}$ slowly increase rDNA copy number up to the proposed threshold required for efficient rRNA production (~35 copies) (French *et al.* 2003; Kim *et al.* 2006). We found a simultaneous return of origin activity to the rDNA locus, but at a lower efficiency than in the parent strain BY4741. We eliminated several possible explanations, including reversion to the wild-type *rARS* sequence, creation of an origin sequence at a new site in *NTS2*, and *trans*-acting mutation elsewhere in the genome. However, closer examination of the sequence of *rARS*$^{GC}$ suggested to us that in the absence of the ACS, a new origin recognition complex (ORC)-binding site (ACS + B1 elements; Figure 8) may have been created fortuitously by the repair template we used (in particular the "B"-PAM site mutation). Its absence in the *rARS*$^{\Delta}$ sequences could explain why no origin activity is associated with *rARS*$^{\Delta}$. However, this hypothesis does not explain why the new origin sequence in *rARS*$^{GC}$ clones remains inactive until the rDNA copy number expands beyond ~10. Two studies from the Diffley laboratory (Santocanale *et al.* 1999; Coster and Diffley 2017) may help explain the gradual return of origin function to the rDNA that we find on continuous culturing of *rARS*$^{GC}$.

First, Coster and Diffley (2017) have refined our understanding of the role of the B2 element in origin function. They recently showed that the B2 element is likely to be a second ACS element and that, with its associated B1 elements, is a binding sites for two ORCs in inverted orientation. In this orientation and spaced ~70-bp apart, they are able to recruit optimally the two head-to-head minichromosome maintenance (MCM) complexes required for origin activation. When the distance between the two B1 elements is reduced to 50 bp, MCM loading *in vitro* drops by 50%, and to 30% when the distance is reduced to 25 bp. In the wild-type *rARS*, the two B1 elements are 31-bp apart, and for the proposed

new ORC-binding site they are only 16-bp apart (Figure 8). If the results from their *in vitro* binding studies hold for the rDNA origin *in vivo*, then this spacing, combined with the less than optimal match to the ACS, may explain the low efficiency of the rDNA origin in the wild-type sequence and its further reduction in the proposed new ACS/B1 sequence. Perhaps the closer spacing is what makes the wild-type *rARS* marginally functional and further reduces the substitute ACS/B1's ability to establish the bidirectional MCM complexes.

Second, Santocanale *et al.* (1999) explored conditions that allow the dormant yeast origin *ARS301* to become active. They found that delay of forks from the adjacent *ARS305* is necessary to see *ARS301* become active, albeit weakly. Moreover, they showed that under these conditions, *ARS301* became active a full 45-min later than *ARS305*. Similarly, Vujcic *et al.* (1999) found that the normally inactive cluster of origins near the left end of chromosome III (including *ARS301*) became active in a strain that carried deletions of *ARS305* (25-kb away) and *ARS306* (59-kb away).

Putting together these two observations from the Diffley laboratory may explain the return of weak origin activity to the rDNA. The replacement of the original ACS with the G+C cassette and the introduction of the D-PAM site mutations have converted what remains of the *rARS* to a dormant origin. When there are ~10 repeats, all of the copies of the dormant *rARS* are passively replicated by the fork coming from the adjacent non-rDNA origin before they have a chance to become active; hence, there are no bubbles on 2D gels. However, during continuous culturing, the pressure to increase growth rate selects for cells that have increased their rDNA copy number. With 15 or 20 repeats, one of the more distal *rARS*s, being further from the incoming fork, has time to fire before it is passively replicated; hence, low levels of rDNA bubbles become visible on 2D gels. This low level of initiation within the rDNA locus, along with the fork from the upstream, non-rDNA origin, could allow maintenance of the marginally expanded rDNA locus.

While we have explanations for some of the phenotypes associated with editing the *rARS*, there are still some interesting questions that remain for future studies. First, *rARS1* and $rARS1^{max}$ are both much more efficient plasmid and chromosomal origins than the wild-type *rARS*; however, when inserted into the rDNA *NTS2*, they are less efficient in that environment than the *rARS* (Figure 1B). What features of chromatin structure, nucleolar location, or transcriptional activity are influencing these origins differently to the native *rARS*? Second, wild-type BY4741 normally has ~150 copies of the rDNA, yet even replacing the *rARS* with $rARS^{"wt"}$, the copy number is very slow to expand and does not reach this large number of repeats even after 150 generations of continuous selection. This result contrasts with the more rapid expansion observed by Kobayashi *et al.* (1998) upon restoration of functional Rpa135 to a W303-derived strain in which the rDNA locus had been shrunk due to loss of Rpa135. Third, how does the status of the *rARS* contribute to fitness and life span? The potential efficiency of the origin in the rDNA is clearly correlated with the ability of the cells to create and maintain ERCs, with a > 100-fold difference between $rARS^{GC}$ or $rARS^{\Delta}$, and *rARS1* or $rARS1^{max}$, yet all of the edited strains have severely shortened life spans regardless of their ERC levels. Perhaps the drastic reduction in rDNA copy number produced by CRISPR/Cas9 editing results in a ribosome deficiency that masks any effects that ERCs or origin efficiency might have on life span. Alternatively, having so few templates for transcription could be creating a burden that interferes with replication or repair of the rDNA, and perhaps it is one of these processes that is responsible for the reduction in life span. Discovering the specific gene, or genes, on chromosome II or IV that increase fitness and/or life span when duplicated will help to resolve these questions. Finally, single-copy origins elsewhere in the yeast genome are individually dispensable. Even the deletion of adjacent origins on chromosomes III (Dershowitz *et al.* 2007) and VI (Bogenschutz *et al.* 2014) causes no obvious growth defects. These findings have led to the conclusion that "no single origin is essential." Yet, we find that deletion of the rDNA origin has profound consequences on fitness and life span by restricting the number of rDNA repeats that can be passively replicated from the adjacent upstream origin, and thus reduces ribosome production. So, is the rDNA origin (considered as a locus) the exception to the rule that "no single origin is essential"? And if the rDNA origin is so critical to rDNA maintenance, then why is the origin inherently so inefficient? What are the evolutionary constraints on ORC and the rARS that drive this suboptimal interaction?

We have shown that CRISPR/Cas9 editing of a tandem repeated locus can be efficient and informative, but we have only edited the origins. Many other interesting functions have been mapped to the rDNA repeats of yeast, both to transcribed and nontranscribed regions. For example, the RFB that enforces the unidirectional traffic of RNA and DNA polymerases in the rDNA has been studied largely by analyzing mutations in Fob1, the protein that binds the RFB and carries out various functions associated with rDNA copy number expansion, recombination, ERC production, and life span determination (Kobayashi *et al.* 1998; Kaeberlein *et al.* 1999; Takeuchi *et al.* 2003). CRISPR/Cas9 technology would make the mutational analysis of the RFB *in situ* a fruitful parallel avenue of study. There are also PolII promoters and transcription units in the rDNA repeats that are well documented, and positioned in interesting places where they may be influencing replication, recombination, sister chromatid cohesion, or PolI transcription (Poole *et al.* 2012; Saka *et al.* 2013). It should now be possible to edit these promoters to assess more completely their roles in rDNA metabolism. Transcriptional silencing by Sir2, and loading of cohesion/condensin in the rDNA, play important roles in many aspects of rDNA metabolism and cell health (Kaeberlein *et al.* 1999; Johzuka *et al.* 2006; Fine *et al.* 2019) that have yet to be fully explored through alterations to the DNA template. In addition, using CRISPR/Cas9 technology it should now be possible to

explore the role of unstructured loops and less-well conserved regions in the rRNAs on ribosome function *in vivo* (for example, Fujii *et al.* 2018). Finally, the technology could be extended to higher eukaryotes to genetically dissect their highly repetitive loci, including rDNA, centromeres, segmental duplications, and other tandemly repeated loci yet to be discovered.

## Acknowledgments

This work was supported in part by the National Institute of General Medical Sciences (NIGMS) (grant R35 GM-122497 to B.J.B. and M.K.R.). M.C. was supported in part by National Institute on Aging (NIA) grants T32 AG-000057 and R01 AG-056359. M.K. was supported in part by NIA grants R01 AG-056359 and R01 AG-056359. M.T. was supported in part by grant R01 AG-056359. A.O. was supported in part by National Human Genome Research Institute grant T32 HG-00035. The research of M.J.D. was supported in part by a Faculty Scholar grant from the Howard Hughes Medical Institute and by NIGMS grant P41 GM-103533. M.J.D. is a Senior Fellow in the Genetic Networks program at the Canadian Institute for Advanced Research.

## Literature Cited

Bahadori, M., M. H. Azizi, and S. Dabiri, 2018 Recent advances on nucleolar functions in health and disease. Arch. Iran Med. 21: 600–607.

Bogenschutz, N. L., J. Rodriguez, and T. Tsukiyama, 2014 Initiation of DNA replication from non-canonical sites on an origin-depleted chromosome. PLoS One 9: e114545. https://doi.org/10.1371/journal.pone.0114545

Boisvert, F. M., S. van Koningsbruggen, J. Navascues, and A. I. Lamond, 2007 The multifunctional nucleolus. Nat. Rev. Mol. Cell Biol. 8: 574–585. https://doi.org/10.1038/nrm2184

Brewer, B. J., and W. L. Fangman, 1987 The localization of replication origins on ARS plasmids in S. cerevisiae. Cell 51: 463–471. https://doi.org/10.1016/0092-8674(87)90642-8

Brewer, B. J., and W. L. Fangman, 1988 A replication fork barrier at the 3′ end of yeast ribosomal RNA genes. Cell 55: 637–643. https://doi.org/10.1016/0092-8674(88)90222-X

Brewer, B. J., C. Payen, S. C. Di Rienzi, M. M. Higgins, G. Ong *et al.*, 2015 Origin-dependent inverted-repeat amplification: tests of a model for inverted DNA amplification. PLoS Genet. 11: e1005699. https://doi.org/10.1371/journal.pgen.1005699

Chernoff, Y. O., A. Vincent, and S. W. Liebman, 1994 Mutations in eukaryotic 18S ribosomal RNA affect translational fidelity and resistance to aminoglycoside antibiotics. EMBO J. 13: 906–913. https://doi.org/10.1002/j.1460-2075.1994.tb06334.x

Chestkov, I. V., E. M. Jestkova, E. S. Ershova, V. E. Golimbet, T. V. Lezheiko *et al.*, 2018 Abundance of ribosomal RNA gene copies in the genomes of schizophrenia patients. Schizophr. Res. 197: 305–314. https://doi.org/10.1016/j.schres.2018.01.001

Chiocchetti, A., J. Zhou, H. Zhu, T. Karl, O. Haubenreisser *et al.*, 2007 Ribosomal proteins Rpl10 and Rps6 are potent regulators of yeast replicative life span. Exp. Gerontol. 42: 275–286. https://doi.org/10.1016/j.exger.2006.11.002

Chiou, L., and D. Armaleo, 2018 A method for simultaneous targeted mutagenesis of all nuclear rDNA repeats in Saccharomyces cerevisiae using CRISPR-Cas9. bioRxiv. Available at: https://www.biorxiv.org/content/10.1101/276220v1.full.

Colombo, S., D. Ronchetti, J. M. Thevelein, J. Winderickx, and E. Martegani, 2004 Activation state of the Ras2 protein and glucose-induced signaling in Saccharomyces cerevisiae. J. Biol. Chem. 279: 46715–46722. https://doi.org/10.1074/jbc.M405136200

Coster, G., and J. F. X. Diffley, 2017 Bidirectional eukaryotic DNA replication is established by quasi-symmetrical helicase loading. Science 357: 314–318. https://doi.org/10.1126/science.aan0063

Defossez, P. A., R. Prusty, M. Kaeberlein, S. J. Lin, P. Ferrigno *et al.*, 1999 Elimination of replication block protein Fob1 extends the life span of yeast mother cells. Mol. Cell 3: 447–455. https://doi.org/10.1016/S1097-2765(00)80472-4

Dershowitz, A., M. Snyder, M. Sbia, J. H. Skurnick, L. Y. Ong *et al.*, 2007 Linear derivatives of Saccharomyces cerevisiae chromosome III can be maintained in the absence of autonomously replicating sequence elements. Mol. Cell. Biol. 27: 4652–4663. https://doi.org/10.1128/MCB.01246-06

Doudna, J. A., and E. Charpentier, 2014 Genome editing. The new frontier of genome engineering with CRISPR-Cas9. Science 346: 1258096. https://doi.org/10.1126/science.1258096

Engel, S. R., F. S. Dietrich, D. G. Fisk, G. Binkley, R. Balakrishnan *et al.*, 2014 The reference genome sequence of Saccharomyces cerevisiae: then and now. G3 (Bethesda) 4: 389–398. https://doi.org/10.1534/g3.113.008995

Faust, G. G., and I. M. Hall, 2014 SAMBLASTER: fast duplicate marking and structural variant read extraction. Bioinformatics 30: 2503–2505. https://doi.org/10.1093/bioinformatics/btu314

Fine, R. D., N. Maqani, M. Li, E. Franck, and J. S. Smith, 2019 Depletion of limiting rDNA structural complexes triggers chromosomal instability and replicative aging of Saccharomyces cerevisiae. Genetics 212: 75–91. https://doi.org/10.1534/genetics.119.302047

French, S. L., Y. N. Osheim, F. Cioci, M. Nomura, and A. L. Beyer, 2003 In exponentially growing Saccharomyces cerevisiae cells, rRNA synthesis is determined by the summed RNA polymerase I loading rate rather than by the number of active genes. Mol. Cell. Biol. 23: 1558–1568. https://doi.org/10.1128/MCB.23.5.1558-1568.2003

Fujii, K., T. T. Susanto, S. Saurabh, and M. Barna, 2018 Decoding the function of expansion segments in ribosomes. Mol. Cell 72: 1013–1020.e6. https://doi.org/10.1016/j.molcel.2018.11.023

Ganley, A. R., and T. Kobayashi, 2007 Phylogenetic footprinting to find functional DNA elements. Methods Mol. Biol. 395: 367–380. https://doi.org/10.1007/978-1-59745-514-5_23

Ganley, A. R., S. Ide, K. Saka, and T. Kobayashi, 2009 The effect of replication initiation on gene amplification in the rDNA and its relationship to aging. Mol. Cell 35: 683–693. https://doi.org/10.1016/j.molcel.2009.07.012

Garrison, E., and G. Marth, 2012 Haplotype-based variant detection from short-read sequencing. arXiv. Available at: https://arxiv.org/abs/1207.3907.

Gibson, D. G., 2011 Enzymatic assembly of overlapping DNA fragments. Methods Enzymol. 498: 349–361. https://doi.org/10.1016/B978-0-12-385120-8.00015-2

He, C., C. Zhou, and B. K. Kennedy, 2018 The yeast replicative aging model. Biochim. Biophys. Acta Mol. Basis Dis. 1864: 2690–2696. https://doi.org/10.1016/j.bbadis.2018.02.023

Hoffman, C. S., and F. Winston, 1987 A ten-minute DNA preparation from yeast efficiently releases autonomous plasmids for transformation of Escherichia coli. Gene 57: 267–272. https://doi.org/10.1016/0378-1119(87)90131-4

Ide, S., T. Miyazaki, H. Maki, and T. Kobayashi, 2010 Abundance of ribosomal RNA gene copies maintains genome integrity. Science 327: 693–696. https://doi.org/10.1126/science.1179044

James, S. A., M. J. O'Kelly, D. M. Carter, R. P. Davey, A. van Oudenaarden *et al.*, 2009 Repetitive sequence variation and dynamics in the ribosomal DNA array of Saccharomyces cerevisiae as revealed by whole-genome resequencing. Genome Res. 19: 626–635. https://doi.org/10.1101/gr.084517.108

Johzuka, K., M. Terasawa, H. Ogawa, T. Ogawa, and T. Horiuchi, 2006 Condensin loaded onto the replication fork barrier site in the rRNA gene repeats during S phase in a FOB1-dependent fashion to prevent contraction of a long repetitive array in Saccharomyces cerevisiae. Mol. Cell. Biol. 26: 2226–2236. https://doi.org/10.1128/MCB.26.6.2226-2236.2006

Kaeberlein, M., M. McVey, and L. Guarente, 1999 The SIR2/3/4 complex and SIR2 alone promote longevity in Saccharomyces cerevisiae by two different mechanisms. Genes Dev. 13: 2570–2580. https://doi.org/10.1101/gad.13.19.2570

Kaeberlein, M., K. T. Kirkland, S. Fields, and B. K. Kennedy, 2004 Sir2-independent life span extension by calorie restriction in yeast. PLoS Biol. 2: E296. https://doi.org/10.1371/journal.pbio.0020296

Kaeberlein, M., R. W. Powers, III, K. K. Steffen, E. A. Westman, D. Hu *et al.*, 2005 Regulation of yeast replicative life span by TOR and Sch9 in response to nutrients. Science 310: 1193–1196. https://doi.org/10.1126/science.1115535

Kim, Y. H., D. Ishikawa, H. P. Ha, M. Sugiyama, Y. Kaneko *et al.*, 2006 Chromosome XII context is important for rDNA function in yeast. Nucleic Acids Res. 34: 2914–2924. https://doi.org/10.1093/nar/gkl293

Kobayashi, T., D. J. Heck, M. Nomura, and T. Horiuchi, 1998 Expansion and contraction of ribosomal DNA repeats in Saccharomyces cerevisiae: requirement of replication fork blocking (Fob1) protein and the role of RNA polymerase I. Genes Dev. 12: 3821–3830. https://doi.org/10.1101/gad.12.24.3821

Kwan, E. X., E. J. Foss, S. Tsuchiyama, G. M. Alvino, L. Kruglyak *et al.*, 2013 A natural polymorphism in rDNA replication origins links origin activation with calorie restriction and lifespan. PLoS Genet. 9: e1003329. https://doi.org/10.1371/journal.pgen.1003329

Kwan, E. X., X. S. Wang, H. M. Amemiya, B. J. Brewer, and M. K. Raghuraman, 2016 rDNA copy number variants are frequent passenger mutations in Saccharomyces cerevisiae deletion collections and de Novo transformants. G3 (Bethesda) 6: 2829–2838. https://doi.org/10.1534/g3.116.030296

Langmead, B., and S. L. Salzberg, 2012 Fast gapped-read alignment with Bowtie 2. Nat. Methods 9: 357–359. https://doi.org/10.1038/nmeth.1923

Larionov, V., N. Kouprina, and T. Karpova, 1984 Stability of recombinant plasmids containing the ars sequence of yeast extrachromosomal rDNA in several strains of Saccharomyces cerevisiae. Gene 28: 229–235. https://doi.org/10.1016/0378-1119(84)90260-9

Laughery, M. F., T. Hunter, A. Brown, J. Hoopes, T. Ostbye *et al.*, 2015 New vectors for simple and streamlined CRISPR-Cas9 genome editing in Saccharomyces cerevisiae. Yeast 32: 711–720. https://doi.org/10.1002/yea.3098

Li, H., 2013 Aligning sequence reads, clone sequences and assembly contigs with BWA-MEM. arXiv. Available at: https://arxiv.org/abs/1303.3997.

Li, H., B. Handsaker, A. Wysoker, T. Fennell, J. Ruan *et al.*, 2009 The sequence alignment/map format and SAMtools. Bioinformatics 25: 2078–2079. https://doi.org/10.1093/bioinformatics/btp352

Liachko, I., R. A. Youngblood, U. Keich, and M. J. Dunham, 2013 High-resolution mapping, characterization, and optimization of autonomously replicating sequences in yeast. Genome Res. 23: 698–704. https://doi.org/10.1101/gr.144659.112

Lin, S. J., P. A. Defossez, and L. Guarente, 2000 Requirement of NAD and SIR2 for life-span extension by calorie restriction in Saccharomyces cerevisiae. Science 289: 2126–2128. https://doi.org/10.1126/science.289.5487.2126

Lowery, R., L. Hung, K. Knoche, and R. Bandziulis, 1992 Properties of I-PpoI: a rare-cutting intron-encoded endonuclease. Promega Notes 38: 8–12.

McGeachy, A. M., Z. A. Meacham, and N. T. Ingolia, 2019 An accessible continuous-culture turbidostat for pooled analysis of complex libraries. ACS Synth. Biol. 8: 844–856. https://doi.org/10.1021/acssynbio.8b00529

McStay, B., 2016 Nucleolar organizer regions: genomic 'dark matter' requiring illumination. Genes Dev. 30: 1598–1610. https://doi.org/10.1101/gad.283838.116

Miller, C. A., R. M. Umek, and D. Kowalski, 1999 The inefficient replication origin from yeast ribosomal DNA is naturally impaired in the ARS consensus sequence and in DNA unwinding. Nucleic Acids Res. 27: 3921–3930. https://doi.org/10.1093/nar/27.19.3921

Mortimer, R. K., and J. R. Johnston, 1959 Life span of individual yeast cells. Nature 183: 1751–1752. https://doi.org/10.1038/1831751a0

Muller, M., R. Lucchini, and J. M. Sogo, 2000 Replication of yeast rDNA initiates downstream of transcriptionally active genes. Mol. Cell 5: 767–777. https://doi.org/10.1016/S1097-2765(00)80317-2

Muscarella, D. E., and V. M. Vogt, 1993 A mobile group I intron from Physarum polycephalum can insert itself and induce point mutations in the nuclear ribosomal DNA of Saccharomyces cerevisiae. Mol. Cell. Biol. 13: 1023–1033. https://doi.org/10.1128/MCB.13.2.1023

Parks, M. M., C. M. Kurylo, R. A. Dass, L. Bojmar, D. Lyden *et al.*, 2018 Variant ribosomal RNA alleles are conserved and exhibit tissue-specific expression. Sci. Adv. 4: eaao0665. https://doi.org/10.1126/sciadv.aao0665

Pasero, P., A. Bensimon, and E. Schwob, 2002 Single-molecule analysis reveals clustering and epigenetic regulation of replication origins at the yeast rDNA locus. Genes Dev. 16: 2479–2484. https://doi.org/10.1101/gad.232902

Pashkova, N., L. Gakhar, S. C. Winistorfer, A. B. Sunshine, M. Rich *et al.*, 2013 The yeast Alix homolog Bro1 functions as a ubiquitin receptor for protein sorting into multivesicular endosomes. Dev. Cell 25: 520–533. https://doi.org/10.1016/j.devcel.2013.04.007

Poole, A. M., T. Kobayashi, and A. R. Ganley, 2012 A positive role for yeast extrachromosomal rDNA circles? Extrachromosomal ribosomal DNA circle accumulation during the retrograde response may suppress mitochondrial cheats in yeast through the action of TAR1. Bioessays 34: 725–729. https://doi.org/10.1002/bies.201200037

Raghuraman, M. K., E. A. Winzeler, D. Collingwood, S. Hunt, L. Wodicka *et al.*, 2001 Replication dynamics of the yeast genome. Science 294: 115–121. https://doi.org/10.1126/science.294.5540.115

Rivin, C. J., and W. L. Fangman, 1980 Replication fork rate and origin activation during the S phase of Saccharomyces cerevisiae. J. Cell Biol. 85: 108–115. https://doi.org/10.1083/jcb.85.1.108

Robinson, J. T., H. Thorvaldsdottir, W. Winckler, M. Guttman, E. S. Lander *et al.*, 2011 Integrative genomics viewer. Nat. Biotechnol. 29: 24–26. https://doi.org/10.1038/nbt.1754

Saka, K., S. Ide, A. R. Ganley, and T. Kobayashi, 2013 Cellular senescence in yeast is regulated by rDNA noncoding transcription. Curr. Biol. 23: 1794–1798. https://doi.org/10.1016/j.cub.2013.07.048

Sanchez, J. C., E. X. Kwan, T. J. Pohl, H. M. Amemiya, M. K. Raghuraman *et al.*, 2017 Defective replication initiation results in locus specific chromosome breakage and a ribosomal RNA deficiency in yeast. PLoS Genet. 13: e1007041. https://doi.org/10.1371/journal.pgen.1007041

Santocanale, C., K. Sharma, and J. F. Diffley, 1999 Activation of dormant origins of DNA replication in budding yeast. Genes Dev. 13: 2360–2364. https://doi.org/10.1101/gad.13.18.2360

Schneider, D. A., A. Michel, M. L. Sikes, L. Vu, J. A. Dodd *et al.*, 2007 Transcription elongation by RNA polymerase I is linked to efficient rRNA processing and ribosome assembly. Mol. Cell 26: 217–229. https://doi.org/10.1016/j.molcel.2007.04.007

Sinclair, D. A., and L. Guarente, 1997 Extrachromosomal rDNA circles–a cause of aging in yeast. Cell 91: 1033–1042. https://doi.org/10.1016/S0092-8674(00)80493-6

Stults, D. M., M. W. Killen, H. H. Pierce, and A. J. Pierce, 2008 Genomic architecture and inheritance of human ribosomal RNA gene clusters. Genome Res. 18: 13–18. https://doi.org/10.1101/gr.6858507

Takeuchi, Y., T. Horiuchi, and T. Kobayashi, 2003 Transcription-dependent recombination and the role of fork collision in yeast rDNA. Genes Dev. 17: 1497–1506. https://doi.org/10.1101/gad.1085403

Tiku, V., C. Jain, Y. Raz, S. Nakamura, B. Heestand *et al.*, 2017 Small nucleoli are a cellular hallmark of longevity. Nat. Commun. 8: 16083. https://doi.org/10.1038/ncomms16083

Torres, E. M., T. Sokolsky, C. M. Tucker, L. Y. Chan, M. Boselli *et al.*, 2007 Effects of aneuploidy on cellular physiology and cell division in haploid yeast. Science 317: 916–924. https://doi.org/10.1126/science.1142210

Vujcic, M., C. A. Miller, and D. Kowalski, 1999 Activation of silent replication origins at autonomously replicating sequence elements near the HML locus in budding yeast. Mol. Cell. Biol. 19: 6098–6109. https://doi.org/10.1128/MCB.19.9.6098

Wai, H. H., L. Vu, M. Oakes, and M. Nomura, 2000 Complete deletion of yeast chromosomal rDNA repeats and integration of a new rDNA repeat: use of rDNA deletion strains for functional analysis of rDNA promoter elements in vivo. Nucleic Acids Res. 28: 3524–3534. https://doi.org/10.1093/nar/28.18.3524

Wang, M., and B. Lemos, 2017 Ribosomal DNA copy number amplification and loss in human cancers is linked to tumor genetic context, nucleolus activity, and proliferation. PLoS Genet. 13: e1006994. https://doi.org/10.1371/journal.pgen.1006994

Wilm, A., P. P. Aw, D. Bertrand, G. H. Yeo, S. H. Ong *et al.*, 2012 LoFreq: a sequence-quality aware, ultra-sensitive variant caller for uncovering cell-population heterogeneity from high-throughput sequencing datasets. Nucleic Acids Res. 40: 11189–11201. https://doi.org/10.1093/nar/gks918

Xu, B., H. Li, J. M. Perry, V. P. Singh, J. Unruh *et al.*, 2017 Ribosomal DNA copy number loss and sequence variation in cancer. PLoS Genet. 13: e1006771. https://doi.org/10.1371/journal.pgen.1006771

*Communicating editor: S. Lacefield*